7-2018

Design and Characterization of an Affordable Laser Communication System

Andrea Tellez
The University of Texas Rio Grande Valley

DESIGN AND CHARACTERIZATION OF AN AFFORDABLE LASER COMMUNICATION SYSTEM

A Thesis

by

ANDREA TELLEZ

Submitted to the Graduate College of
The University of Texas Rio Grande Valley
In partial fulfillment of the requirements for the degree of

MASTER OF SCIENCE

July 2018

Major Subject: Physics

DESIGN AND CHARACTERIZATION OF AN AFFORDABLE LASER COMMUNICATION SYSTEM

A Thesis
by
ANDREA TELLEZ

COMMITTEE MEMBERS

Dr. Volker Quetschke
Chair of Committee

Dr. Teviet Creighton
Committee Member

Dr. Mario Diaz
Committee Member

July 2018

ABSTRACT

Tellez, Andrea, Design and Characterization of an Affordable Laser Communication System . Master of Science (MS), July, 2018, 71 pp., 13 tables, 57 figures, references, 57 titles,

Over the last decades, an exponential growth in communication demand has been observed. Radio Frequency (RF) band has been one of the most used bandwidths for data transmission in the world. Given the influence and the continuous growth of communication technology, the RF spectrum is overpopulated. More efficient systems are necessary to meet the communication needs of this generation. A change to optical bandwidth is the most practical alternative to deal with the congestion of radio frequency.

The aim of this thesis is to present the features of Free Space Optical links with off-the-shelf components. A description of how these systems can apply to satellite communication is given. A theoretical background of the history of optical communications will be provided followed by a gander at the fundamental properties of FSO mechanisms. The thesis will conclude with a detailed description of the choice of hardware utilized, results, and future work.

DEDICATION

This thesis is for all women who have and will support me through this journey, who had been and will be my role models, and to the upcoming scientists that will be inspired by my dedication in this field. Representation matters.

ACKNOWLEDGMENTS

I want to acknowledge and thank for the endless support from my research advisor, Dr. Volker Quetschke. During these past six years, from my undergraduate and graduate studies, he has guided me to be a successful scientist and I will always be grateful for that. I also want to thank the rest of my thesis committee for their time and guidance, Dr. Teviet Creighton, and Dr. Mario Diaz.

TABLE OF CONTENTS

Page

LIST OF TABLES

Page

LIST OF FIGURES

Page

CHAPTER I

INTRODUCTION

The aim of this section is to first provide a theoretical grounding of the physics involved in the setup before discussing the design, construction and equipment details as well as principles of operation and optimization procedures.

1.1 Brief History of Free Space Optical Communications

The use of light as a form of communication has been present since centuries ago. Civilizations first methods of optical transmission were through mirrors, smoke signals, and fire beacons. Since AD 26-37, the Roman emperor Tiberius from the island of Capri took advantage of the sun by reflecting its light with metal mirrors to send messages. Another popular method was the use of smoke signals in ancient Asia during the 8th century. The Great Wall's soldiers utilized this technique to alert the army from the enemies. Other civilizations also used them to announce war's victories. Smoke signals were that practical that around 150 BCE the Greeks created a communication system. They converted alphabetic characters into numeric characters improving this method drastically, even today they are still used. However, the signal transmitted was limited and like nowadays, the need for more advanced techniques was needed.

It was not until 1792 when the French inventor Claude Chappe made a major advance in communication networks. He came up with a code scheme to transmit long-distance messages via a mechanical device known as the semaphore telegraph. In 1794 the first successful message using this device was sent from Paris to Lille, two cities 200 km apart. To have a better understanding of the data rate of this system the bit is the smallest unit of information in a binary system; the rate of the telegraph was less than a bit per second. The use of Morse code increased this rate and with

help of relay stations, the line reach increased to 1000 km.

Almost a century later, in 1880's one of the most practical and revolutionary ways of communication was built: the telephone. Patented by Alexander Graham Bell and Thomas A. Watson in 1876, this device converted acoustic waves to electrical signals and transmitted the voice signal over a distant location. The first clear transmission was established on March 10, 1876, where Bell spoke into the device, "Mr. Watson come here, I want to see you" and Watson was able to reply back. From that day until now, telephones have indispensable for human life.

Thereafter, since 1980's National Space agencies investigated the possibility to relay data from a low earth orbiting satellite to the ground via a geostationary satellite through a high data rate optical link.

1.1.1 The SILEX mission

In 1991, the Centre national d'etudes spatiales (CNES) and the European Space Agency (ESA) started to collaborate for an optical communication system. In November 2001, this two agencies implemented the Semiconductor Inter-Satellite Link EXperiment (SILEX), a terminal in space. SILEX was the first successful inter-satellite laser communication link in history. This laser communication link comprised two optical terminals: PASsager TELecom (PASTEL) and Optical PAyload for Inter-Satellite Link Experiment (OPALE), aboard two satellites: SPOT-4 and ARTEMIS, respectively. PASTEL was the optical terminal aboard the French Earth Observation Satellite, SPOT-4, and OPALE was on the ESA geostationary satellite, ARTEMIS. SILEX established four data links, lasting 4 between 20 minutes, with a data rate of 50 Mbps [2]. The Artemis satellite was in a parking orbit at 31,000 km (GEO) moving around 7000 mph while the SPOT-4 satellite was orbiting at an altitude of 832 km (LEO) at 16,600 mph. During the data link communication the two satellites had an average distance between them of 38,500 km. The bit error rate for this space link was reported to be consistent between 10^9 to 10^{10} [1].

Figure 1.1: SILEX communication link [2]

Then in 2005, the Japanese Optical Inter-Orbit Communications Engineering Test Satellite (OICETS) and ARTEMIS demonstrated a bi-directional optical link [3] [4]. This is the second successful optical data relay after SILEX. Optical data relays improve the way of transmitting data around Earth. Science applications, earth observations, space operations, and telecommunication services benefit from this technology. Using optical links provide higher data rates, secure and free interference links with low mass and power terminals to space systems. Three years later, a connection between Terra SAR-X and NFIRE, two LEO orbiting satellites was demonstrated. The two LEO satellites achieved a data transfer of 5.5 Gbps over a total distance of 5500 km at a 25000 km/h speed. Then the first ground-satellite optical link was successfully conducted between the optical ground space (OGS) and (Engineering Test Satellite-VI) ETS-VI satellite in Konegi, Japan [6], [7].

Military and aerospace laboratories also performed several successful experiments with various optical network setups. Some ground-to-satellite, satellite-to-satellite and satellite-to-ground successful missions were: the airborne flight test system (AFTS), laser cross-link system (LCLS), optical communication demonstrator (OCD), stratospheric optical payload experiment STROPEX (CAPANINA Project), Mars laser communications demonstration (MLCD), and airborne laser optical link (LOLA).

The AFTS comprised a link between a ground station in New Mexico and an aircraft [8] while the LCLS was a geosynchronous system with a full duplex space-to-space link [11]. Another

satellite-to-ground mission is the OCD. OCD was developed in a laboratory to demonstrate high-speed data transfer. The CAPANINA project was a high bit-rate optical downlink from the airborne station to an optical ground station [12], the MLCD provided up to 10 Mbps data transfer between Earth and Mars [13], [14], and LOLA was the first demonstration of a two-way optical link between a high altitude aircraft and GEO satellite ARTEMIS [15], [16].

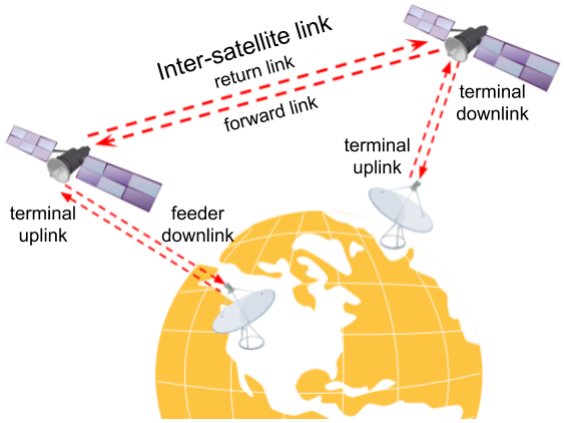

Figure 1.2: Optical communication link arrangements.

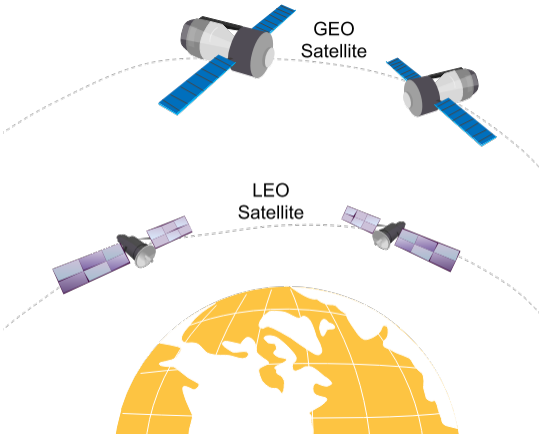

Figure 1.3: Inter-satellite links orbiting LEO and GEO.

1.2 CUBESATS

In the course of the last decade, satellite systems have grown to be an essential element for modern communications. Small satellites are among the quickest developing classes of satellites due to their low-cost components, short development time, and launch opportunities. Figure 1.4

demonstrates the number of small satellites propelled from 2000 to 2013, many satellites with a mass of 1-50 kg have been propelled with a noteworthy increment in the satellites that weight 1-10 kg. A steep increase is expected in the upcoming years [33]. Among those small sats, a large part are CubeSats, a strict size, and weight modular cube satellite that piggy-back on bigger launches [34]. With the growth on demand for services, especially for mobile communication, TV, and Internet, these systems are in ceaseless advance. Therefore, considerable ventures are being made at the governmental and educational level, to address the progressing advancements in these sectors [35].

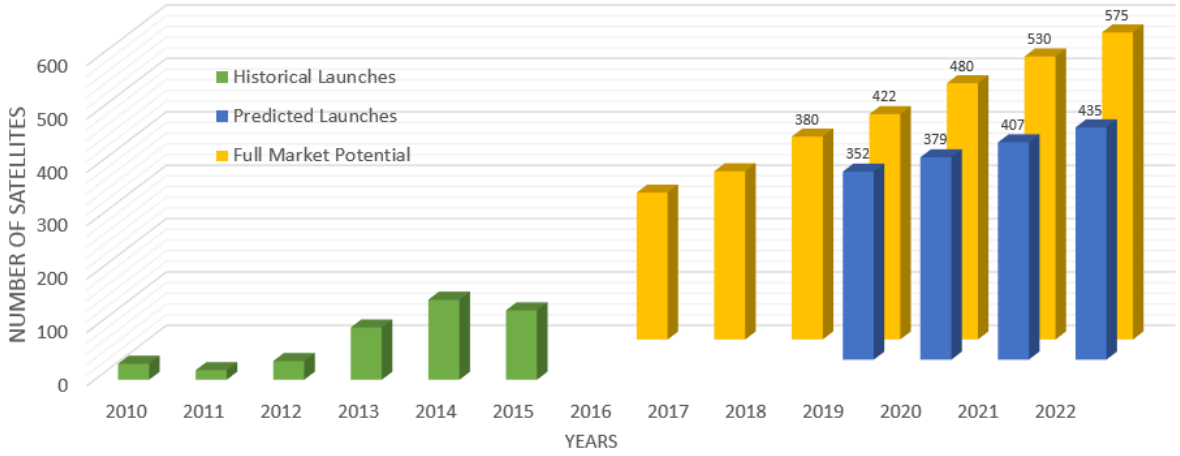

Figure 1.4: Number of nanosats, microsats, and satellites launches that weight 1-50 kg [36].

A crucial factor of any satellite system design is the infrastructure of the transmission system. The overall performance of a mission is directly impacted by the capabilities of the communication link subsystem. These constraints are particularly noticeable on resource-constrained satellites such as CubeSats [37]. One CubeSat unit has a 10x10x10cm volume and a 1.33 kg weight constraint. Experiments consist of 1U, 1.5U, 2U, and 3U (Figure 1.5).

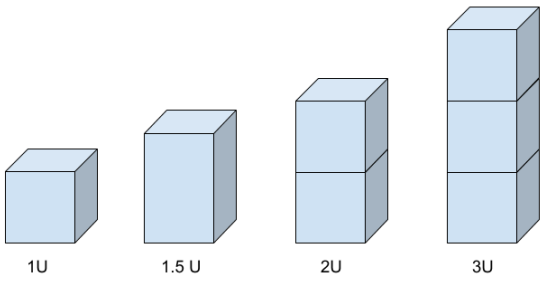

Figure 1.5: Common sizes used for cubesat experiments.

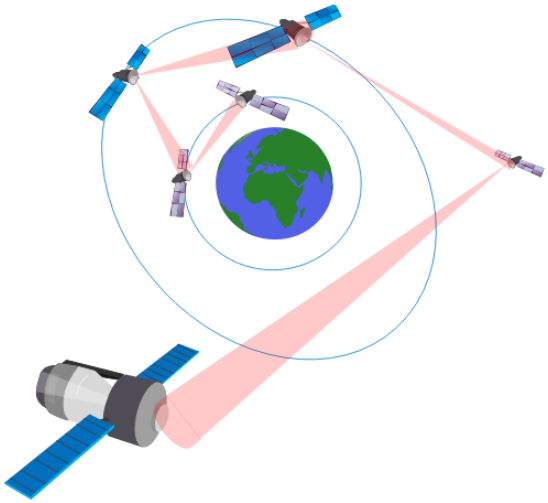

Figure 1.6: Satellite-to-Satellite Links.

CubeSats have the advantage to perform all the standard functions of a common satellite. These functions are attitude control, up and down communication links, onboard data management, storing information on a CPU, the addition of sensors or/and a camera, among others. They can also include solar panels or/and antennas.

CubeSats have a wide range of scientific applications and democratize the access to space. Thus, this thesis studies the design of a laser communication system using these cost-effective, fast communication small satellites.

1.3 Thesis Overview

This thesis starts with a brief history of the usage of light as a way to communicate. Followed by some background of the first FSO systems implemented for space applications. The primary

focus of this thesis is to apply laser communication system to small satellites by using off-the-shelf components. Chapter II gives an extensive review of the features and advantages of using an optical source for satellite communication over RF technology. These advantages include the bandwidth, spectrum use, bit error rates, the communication link security, and data rates. This will be followed by a description of some FSO ground applications. In addition to a section discussing the acquisition, pointing and tracking for controlling the beam of the system.

Limitations and challenges of the system such as atmospheric effects are given in Chapter III. Chapter IV describes the choice and mechanisms of every component used in our system as well as the main concepts that are necessary to design a laser comm system. This chapter aims at providing the necessary theoretical basis for understanding the principle of operation of the experimental setup. The hardware and operation of the experiment are given in chapter V.

The results of the system analysis varying the frequency modulation with two different setups are presented in Chapter VI. The last section in this thesis is a conclusion and future work detailing the phases that must follow for the optimization and development of an affordable high bandwidth communication system between small satellites using lasers.

CHAPTER II

LITERATURE REVIEW

Over the last decades, an exponential growth in communication demand has been observed. Since 1864 that Maxwell predicted the propagation of electromagnetic waves through free-space and Hertz transmitted radio waves in his lab in 1880; Radio Frequency band (RF) has been one of the most used bandwidths for data transmission in the world. In consequence, the RF spectrum is overpopulated by mobile communication services, television, radio, the Internet, among other communication systems. RF does not meet the necessary requirements anymore to tackle the ever-growing communication technology. Hence, the need to shift to the optical bandwidth. A change to optical bandwidth is the most practical alternative to the congested radio frequency and microwave bands. These electromagnetic regions provide unique features that will be discussed along this thesis work.

2.1 Optical Bandwidth

The optical bandwidth is the name given to the range of frequencies (wavelengths) used for optical communication systems and is divided into regions. Currently, the majority of the optical systems operate in the near-infrared wavelength region (780 nm to 850 nm), mostly due to its cost advantages and availability of effective and reliable semiconductor laser diode sources at that wavelength region. Although cost is undoubtedly a significant factor in the choice of wavelength, one must analyze several additional constraints, like the need to not exceed eye-safe limits. Other relevant criteria include overall performance and the potential for system growth and versatility. When all of these factors are considered, it becomes evident that a more exhaustive approach is to operate near 1550 nm, the same wavelength range employed in commercial fiber-optic

communications networks.

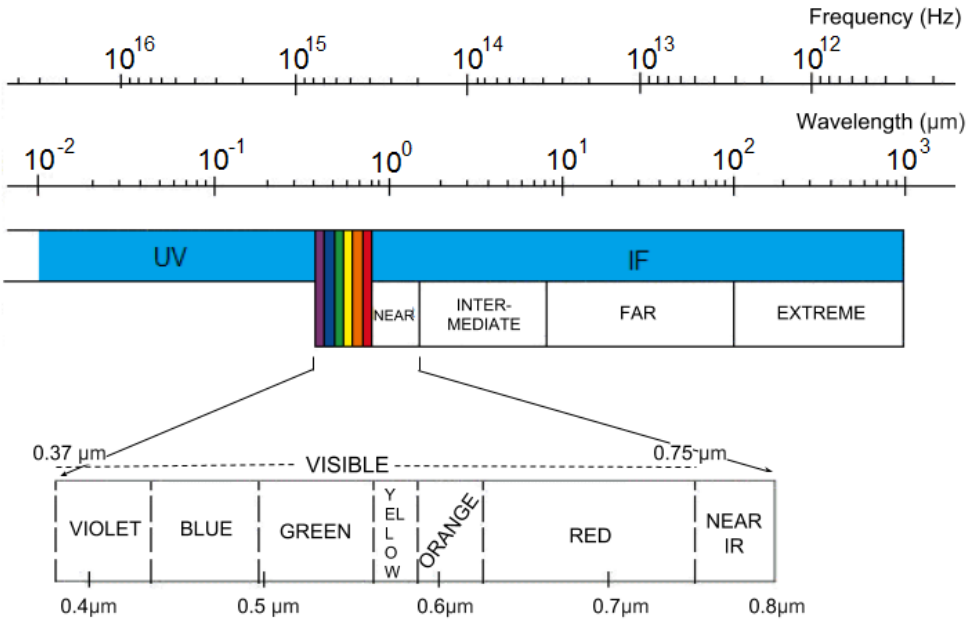

Figure 2.1: Optical band.

2.2 Free Space Laser Communication in Space

A basic Free Space Optical (FSO) communication link consists of an optical source to wirelessly transmit data through an unguided channel, a few optics, and a receiver to gather/detect the emitted information signal (Figure 2.2). Optical wireless links offer a promising fast, secure, and reliable high bandwidth alternative to RF communication links by taking advantage of the high directionality of a narrow laser beam. This ensures that most of the transmitted power will be used for communication thus achieving high-efficiency long-reach links.

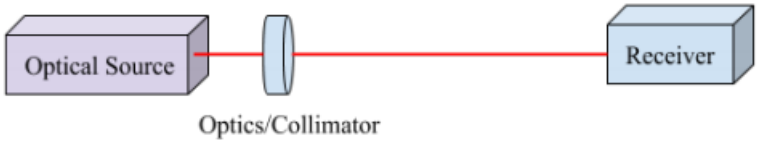

Figure 2.2: Scheme of a basic free space optical communication link.

The optical sources used in FSO communications are often in the near infrared (IR) (800-2500 nm) and visible band (390-700 nm), within the atmospheric window (Figure 2.1) to establish

a terrestrial link (building-to-building) or space optical links (ground-to-satellite, inter-satellite and deep space). FSO links can also be bi-directional, meaning that they can transmit and receive data simultaneously. Hence, several transmitter/receiver link configurations are possible (Fig. 1.2 and 1.3).

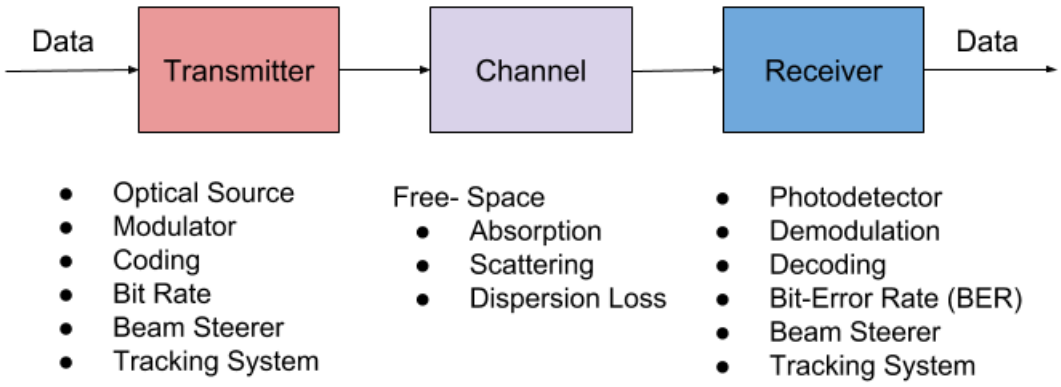

Figure 2.3: Block diagram of a free space inter-satellite optical communication link .

2.2.1 Beam Control

To establish an FSO in space, an Acquisition, Tracking, and Pointing (ATP) system must be considered. Such system points the optical signal towards the required target(s) (e.g. to the receiver or emitter) and locks the laser on the targets despite disturbances caused by the movement of the target, atmospheric instability, or random jitter. An acquisition, pointing and tracking systems have been effectively executed in numerous applications ranging from short-distance cases, for example, motion tracking, to long-distance applications such as rocket guidance systems.

The principles of operation of an ATP system design depends on the application. As illustrated in 2.3, an FSO-Space Link first modulates the data from the transmitter onto an optical carrier, a laser, then the laser beam is collimated through an optical system and transmitted as an optical field into the atmospheric channel. One requirement of an ATP system is to incorporate a beam steering into the design, which transforms the transmitter into a beam steerer. The beam scans the region of space where the receiver's expected location, to reduce the time of acquisition, the beam requires a wide beam and hence a high power optical transmitter [6]- [13]. At the receiver, the arriving optical field is first collected through an optical front-end and projected onto a photodiode

for signal detection. One big problem faced by communication links in space is to establish a steady link between the satellites, due to their vibrations and relative velocity.

2.3 Advantages of Free Space Optical Communication in Space

FSO has demonstrated its capability to deliver data faster than any other cutting-edge communication technology. There are several significant features and advantages of FSO communications over RF-based wireless systems. These advantages are enabled by the laser narrow beam-width that leads to a stable, secure link, higher data rate, and high communication bandwidth with fewer spectrum regulations [38].

2.3.1 Narrow beam divergence

An optical source posses a narrow beam divergence made possible by the diffraction property of electromagnetic waves. The theoretical diffraction limit states that the directionality of a beam with a Gaussian energy profile is described by the laser beam wavelength and the aperture diameter [39]. Since the wavelength of the optical carrier used in laser communication is in the order of microns (substantially shorter than RF wavelengths), laser beams can achieve a divergence angle orders of magnitude narrower than RF beam-widths. The following equation expresses the half-angle divergence of a Gaussian beam TEM_{00} (for more details refer to section 4.1.3),

$$\theta \approx \frac{\lambda_{carrier}}{D_{aperture}} \tag{2.1}$$

where $\lambda_{carrier}$ is the wavelength of the carrier and $D_{aperture}$ is the diameter of the receiver's aperture.

The narrow beam divergence of the signal offers a major advantage for space optical systems as it prevents the dissipation of the transmitted power along the communication link. Additionally to this advantage, a narrow beam laser has very reliable and stable channels with a low probability of interception that improves the signal-to-noise ratio (SNR) of the received signals, therefore, enhances the bit-error-rate (BER).

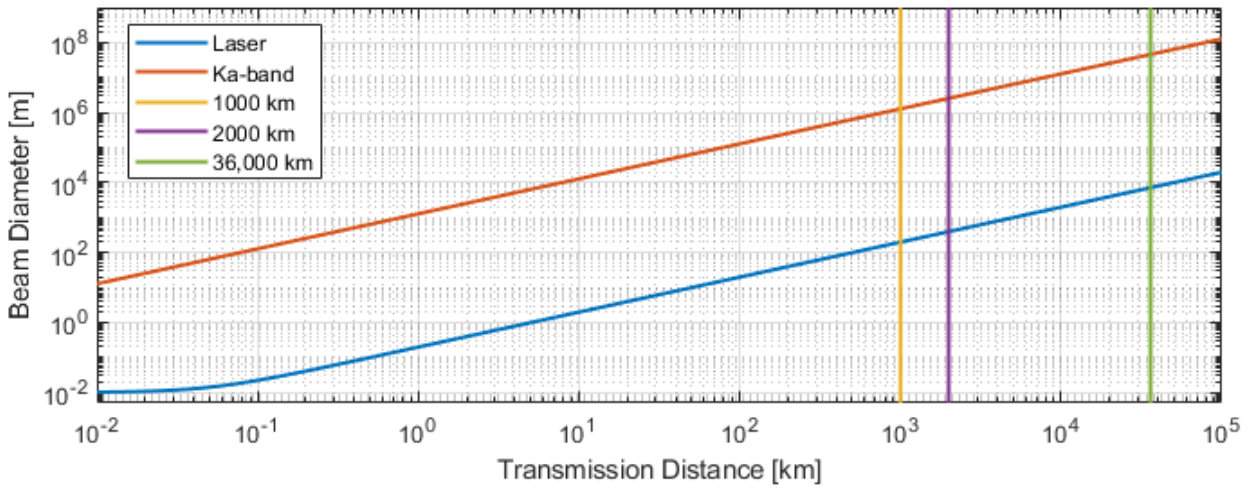

Figure 2.4: Beam diameter as a function of link distance with a 1-cm emitter diameter.

Figure 2.4 shows the beam diameter of a laser communication system as a function of link distance for a 1-cm diameter transmitter. The graph compares a 1550-nm and a Ka-band (30 GHz) link. Three distances are plotted for comparison. The first line is at 1000-km which is the future design distance goal, the second line is the distance from Earth to the Low Earth Orbit (LEO), one of the desired configuration links to accomplished as well as a Geostationary Orbit (GEO) communication link. Refer to table 2.1 to see the beam diameter and relative power values for different configuration links.

Type	RF	Optical
Transmission Distance	1000 km	
Beam Diameter	1280 km	0. 198 km
Relative Power Detected	$6\text{x}10^{-17}$	$2.5x10^{-9}$
Transmission Distance	2000 km	
Beam Diameter	2,540 km	0.395 km
Relative Power Detected	$1.53\text{x}10^{-17}$	$6.4\text{x}10^{-10}$
GEO		
Transmission Distance	36,000 km	
Beam Diameter	45,500 km	7.1 km
Relative Power Detected	$4.76\text{x}10^{-20}$	$1.95\text{x}10^{-12}$

Table 2.1: Different link configurations for a 1-cm emitter and receiver diameter.

2.3.2 Power and Mass Efficiency

Subsequently, optical systems with a laser source offer a higher beam directionality, thus reducing the required optical power by the implementation of smaller transmitter and receiver apertures. The relative power detected as a function of transmission distance is shown in Figure 2.5.

Again, we compare two systems, one at 1550-nm laser and another source using a Ka-band. If we look at the power at the 1000-km transmission distance, the relative power using the laser as the light source goes down to approx $2.5\text{x}10^{-9}$. Assuming a 10-mW laser power, the detected power will result in 25-pW. To have a better idea, one pW is a human cell mean power consumption and 150-pW is the power detected by a human eye from a 100-W lamp 1 km away. A 1550-nm laser with this amount of power doesn't cause retinal damage. However, the value can be improved when the light is transmitted in a dispersion-free environment like a vacuum or in space (aka a perfect vacuum). From figure 2.5 we can also see that power values are worst employing RF technologies.

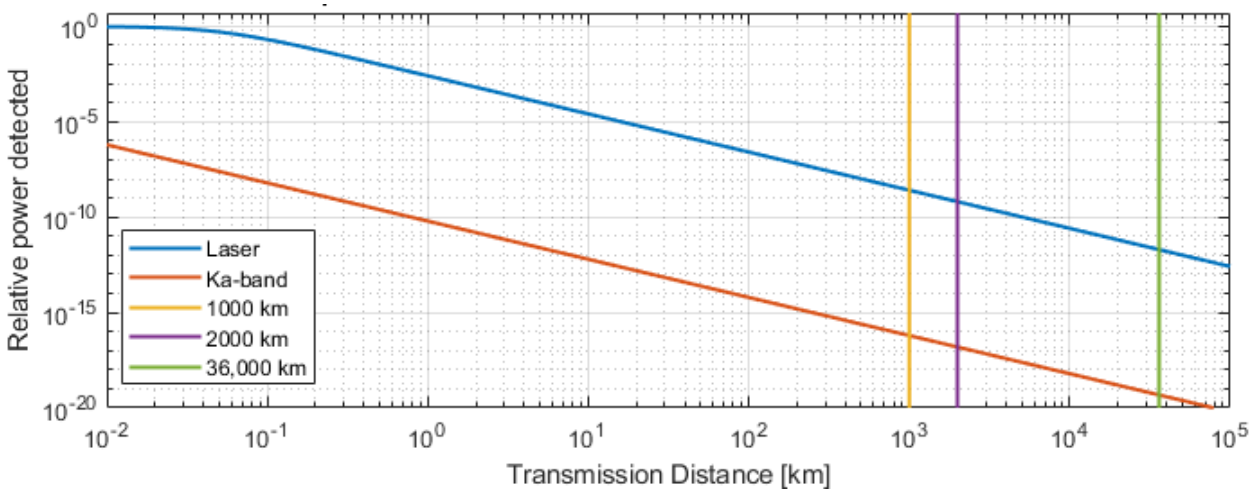

Figure 2.5: Fraction of power received over link distance with a 1-cm receiver diameter.

2.3.3 Higher Data Rates

Optical information transmission has been revealed to be an auspicious and low-cost approach to send high rate information data streams. FSO systems have the potential of significantly reducing the timeline for delivering information and enabling new applications that require fast transmission channels (e.g. sending high-resolution videos). The speed of a given transmission

channel, called data rate, is measured by the number of bits transmitted in a second. High data rates require a lot of spectrum. Thus, higher frequencies enable higher data rates. For example, at Ka-band the frequency bandwidth is usually 500 MHz for frequencies around 38 GHz. In contrast to optical systems, the bandwidth can be 1000 times larger at 1550 nm, carrying considerably more amount of data.

The only way RF systems can compete with these data rates is through modulation which is not power nor mass efficient for the system design. This amount of bandwidth can be used to carry an enormous amount of information, but the usefulness of this bandwidth will be limited by factors such as the ease with which information can be imposed upon the beam, the ability for the channel to support it and the capability of the receiver to detect and decode it. These factors will be described in subsequent sections on modulation and demodulation techniques and channel effects.

2.3.4 Unlicensed spectrum

Wireless networks, mobile phones, radio stations, air-traffic control, and even astronauts rely on radio waves to communicate. The radio spectrum is overcrowded and the increase of communication systems plus the inability of radio spectrum to be expanded, it is demanding a switch to other bandwidths. Also, RF systems fear an increase in price in the close term, in view of supply and demand.

The radio spectrum is the world's natural frequency resource and it is required to be well-managed. In order to not interfere with each RF systems, the International Telecommunication Union (ITU) controls the implementation of radio frequencies throughout the world. Countries must follow the assignments specified in the ITU Radio Regulations' Article S5 (International Table of Frequency Allocations). In 2000 at the World Radio Communication Conference (WRC-2000) the ITU expanded the radio regulations from 400 GHz to 1000 GHz (1 THz) but ITU still does not regulate frequencies in the optical spectrum (above 3 THz).

Most countries regulate the employment of radio frequencies by requiring that the usage of these frequencies be licensed. In the USA, the Government Interchanges Commission (FCC) issues these licenses. Acquiring a license may include multiple hardware tests (for intentional

and inadvertent radiations), examinations for administrators, and a permit charge which pays for a license that will be valid for a pre-defined number of years. FSO frameworks that have been deployed are as yet rare, and the highly directional nature of optical transmissions suggest that issues of obstruction would be highly uncommon. Although, FSO links also need some type of control not managing the use of spectrum but instead, from a safety viewpoint. Laser safety is administered universally by the International Electrotechnical Commission (IEC), while inside the United States, the Center for Devices and Radiological Health (CDRH) and the American National Principles Organization (ANSI) guarantee item and client security individually. Laser safety will be examined in section 4.3.3.

2.3.5 High Security

Radios signals can be disturbed by employing electronic counter-measures (ECM) to detect the presence of these signal transmissions. Prior to the high-quality data and security techniques of now, enemies seized advantage of ECM during wars. The enemies demodulated and decoded the signals for intelligence and counterintelligence purposes. Basic radio systems can be manipulated to provide false information but even employing high-quality security techniques, the signal can be disrupted or/and exploited. This is possible by employing a basic radio direction finding (RDF) or position monitoring. A diagram with basic ECM techniques is shown in Figure 2.6.

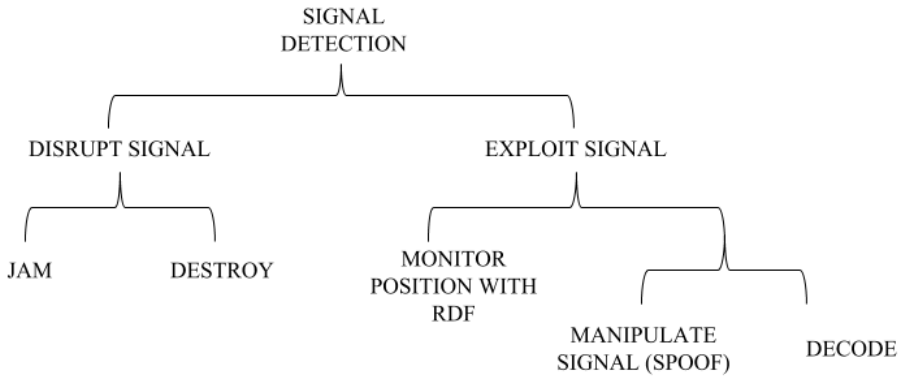

Figure 2.6: Basic diagram of Electronic countermeasures (ECM).

The traditional approach of detecting an RF transmission is through spectrum analyzers or RF meters. However, this equipment cannot be used to detect laser transmissions. To detect a laser

communication, a compatible FSO receiver or some form of electro-optical system is needed to convert the optical frequencies to electrical signals. Thus, any sort of interception along these lines is extremely difficult. There are two places in which a laser beam can be detected. Firstly, it can be detected from within the beam. The beam divergence determines the probability of detection from within the beam. Secondly, the beam may be "seen" from outside the beam. In this case, the "visibility" of the beam determines whether it can be detected. This will be discussed further in the section 4.1.4 about beam divergence.

2.4 FSO Ground-based Communications

FSO is also an alternative for ground-based communications.

2.4.1 Advantages and Opportunities

- **Li-Fi:**

  In 2011, the German physicist Harald Hass proposed a new technology called Light Fidelity (Li-Fi). This innovation is a wireless optical network that uses light-emitting diodes (LEDs) for transmission of data. The basic principle behind this technology is to transmit information through a wireless medium with LED light by varying the intensities of the light source very fast (the operating speed of LEDs is slighter than one microsecond), similar to Wi-Fi [10].

  Li-Fi can be used for vast of applications, from public Internet connection through existing lighting (LED) to vehicles that can use their headlights (LED-based) to communicate. Applications of Li-Fi can extend in areas where Wi-Fi lacks its presence like aircrafts, power plants, radio-free zones (e.g. Green Bank, West Virginia) and various other areas, where electromagnetic (Radio) interference is of major concern for the safety of people and equipment (e.g. Green Bank telescope).

2.4.2 Direct laser communication on earth

Earth systems using lasers to communicate have the disadvantage of dealing directly with weather, see next section on Atmospheric effects. The advantages are that you're free from dealing with cables and obtaining a highly directional signal. There are various opportunities for

high bandwidth connections. Less infrastructure is needed resulting in low costs, benefiting big production plants.

CHAPTER III

LIMITATIONS AND CHALLENGES

3.1 Atmospheric Effects

Since FSO communications propagating medium is an unguided channel (e.g. air, vacuum), this technology is subject to atmospheric effects. FSO communication systems are dependent on weather and geographical location. Multiple factors like fog, rain, snow, humidity, and haze, cause high attenuation in the signal and limits the link's performance. As the laser beam propagates through the air the signal is attenuated. Among these constraints, factors like background noise, pointing, and link availability also limits the signal. This segment will discuss some challenges faced by different system designs in ground-to-satellite/satellite-to-ground links as well as inter-satellite links.

3.1.1 Ground-to-Satellite and Satellite-to-Ground Links

Ground-to-satellite and satellite-to-ground FSO signals encounter the Earth's atmosphere. The losses during FSO ground-to-satellite systems are astronomical compared to satellite-to-ground links. That is because as the optical signal is emitted from the ground station, the source beam begins to spread and accumulate distortion until it reaches the satellite.

When a laser beam propagates through the atmosphere, it experiences power loss due to diverse factors; it is essential to examine rigorously the system design requirements to tackle the unpredictable changes from the atmosphere. The optical beam also changes in distinct ways depending on the altitude. The main changes are corresponding to variations in temperature, pressure, the concentration profile of various atmospheric constituents, and aerosol particles. Just above the Earth's surface, 1-2 km, the largest concentration is encountered. Refer to [13] [15]

for simulations of atmospheric transmittance and background sky radiance for various altitudes, aerosols distribution, among others. To achieve a stable and reliable laser communication system in free space, it is required to have a deep understanding of how the optical beam propagates through unpredictable transmission mediums (e.g. the atmosphere) and their losses. Various losses experienced by the optical beam when propagating through the atmospheric optical channel are:

3.1.2 Absorption, Scattering, and Dispersion Loss

In an FSO system, different gases and aerosol particles found in the Earth's atmosphere interacts with the laser beam and drastically absorb the signal. The loss in the unguided channel is generally due to absorption and scattering of the optical source. For more information about various conditions of the propagation of the laser in the atmosphere, refer to [17]. At visible and IR wavelengths, the main atmospheric absorbing particles are water, carbon dioxide and ozone [18], [19].

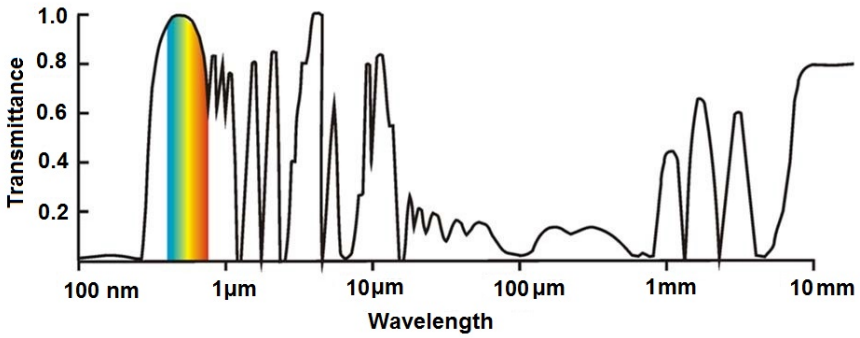

Figure 3.1: Transmittance of Electromagnetic Radiation across the spectrum [20].

Absorption is when the energy of the optical source is lost due to the atmosphere at a molecular or atomic level. The atmospheric absorption phenomenon depends on the wavelength. In the visible light portion, ozone and oxygen gases slightly absorb the signal. The portion used for FSO systems remains between 700-1500 nm (near-IR), water molecules are the absorbers that predominate at these frequencies. The wavelengths above 1500 nm are operated by microwave and radio technologies and affected primarily by water and carbon dioxide. High atmospheric

transmittance values are the main reason for the choice of wavelength.

The atmospheric transmission window is the range of wavelengths for FSO communication with a minimal absorption (attenuation less than 0.2 dB/km). There exist multiple transmission windows within 700 and 1600 nm. FSO systems are commonly designed to operate in the 780-850 nm and 1520-1600 nm window. These wavelengths have the advantage of available components for the transmitter and receiver. Simulations of the attenuation under different weather conditions as a function of wavelength are available in databases [21], [22].

Another agent that degrades the performance of the system is the scattering of light. Scattering is a physical phenomenon where the direction, frequency, or polarization of a wave produced by an optical source change. This is happens when the wave travels to a medium and encounter certain discontinuities in the transmittance channel. Just like absorption, scattering strongly depends on wavelength.

Scattering is divided into three categories, depending on the size of the atmospheric particles (the scatterer): molecular scattering (Rayleigh scattering), aerosol scattering (Mie scattering), and geometrical scattering (Non-selective scattering). If the optical wavelength is greater than the size of the atmospheric particles, then Rayleigh scattering is produced. Rayleigh scattering is generated by air molecules and haze; it is also dominant at wavelengths below 1000 nm (visible/near IR range). However, it can be neglected at longer wavelengths near IR range [23]. In the case that the optical wavelength is comparable (or larger) than the size of the atmospheric particles, then Mie scattering is produced. The main contributors to Mie scattering are aerosol particles, fog, and haze. At near IR wavelength range (or longer) this scattering is prominent. For the third type of scattering, the value of the optical wavelength is lower than the atmospheric particles. In this case, the scattering is better described by geometrical optic models [24], [25].

Additionally, ground-to-satellite transmissions are altitude-dependent. The atmospheric transmittance is increased at high elevation angles because the impact of aerosols particles is reduced.

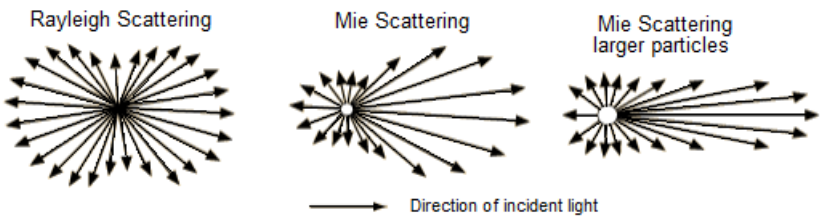

Figure 3.2: Illustration of scattering types. [57]

Mitigation techniques can be employed to optimize the communication links in the atmosphere. However, outer space has no dispersion due to its low pressure and density. Hence, it's perfect to establish a stable laser communication system.

CHAPTER IV

RESEARCH METHODOLOGY

4.1 System Architecture: Optical Source

For laser communications, there are different devices used as the optical carrier such as LEDs (Light Emitting Diodes) and lasers. Lasers are classified according to the lasing medium used to generate their signal. These classifications are: gas (chemical and excimer lasers), solid state (fiber hosted, photonic crystal, and semiconductor lasers), dye, and free electron lasers. The firsts FSO systems started using Gas lasers as their transmitter source. However, their lasing medium (chemical substances) degrades over time, decreasing its efficiency to generate a constant output power signal. On the other hand, we have solid-state lasers, which are unique for its compactness and robust design. Although, the power consumed is less than the one for gas lasers they still require a high current value to be able to operate.

The surge of semiconductor laser diodes origin in the early 1960s, not long after the development of other laser systems innovations. Semiconductor lasers are a technology that has revolutionized the world we live in. Semiconductor laser diodes are arguably the most important of all lasers due to their wide variety of applications, ranging from optical frequency standards [40],[41], tests of relativity [42], generation of low-phase-noise microwave signals [43], and transfer of optical stable frequencies by fiber networks [44], to gravitational wave detection [45]. They have well-known features and characteristics like high reliability, miniature size, lower power consumption, wide tunability, high efficiency, and excellent direct modulation capability. Currently, solid-state lasers are the most used in space optical communications.

Parameter	Laser	LED
Wavelengths Available	780-1650 nm	600-1650 nm
Spectral width	Narrow (1x10^5 to 10 nm FWHM)	Wide (40 to 190 nm FWHM)
Output power	High	Low
Bandwidth	High	Moderate
Numerical Aperture	Small	Large
Cost	More $500	$5 - $300
Speed	Faster	Slower
Ease of Operation	Harder	Easier

Table 4.1: Comparison between a Laser beam and a Light Emitting Diode for communication links.

The choose of the laser depends primarily on the required wavelength and output power signal. Lasers are able to establish a secure and stable link thanks to the narrow, high directive laser light beam and it is well-defined wavelength, the emission of monochromatic radiation. These specific characteristics are needed to ensure link safety, reduce the degradation of the laser' beam, and facilitating modulation at high data rates. LEDs are used as well for free space-comm. A comparison between lasers and LED is given in table 4.1.

4.1.1 Optical Requirements

One of the most important parameters on the design of FSO systems is the wavelength of the optical carrier. It is a crucial part, as it plays a key role in the performance and capacity of the system as a whole. Mostly, affects the quality of the link and the receiver's sensitivity.

4.1.2 Choice of Wavelength

Choosing the wavelength depends predominantly on the attenuation, noise power, and atmospheric effects. In addition to the accessibility of the transmitter and receiver components, the cost, and eye-safety regulations impact this selection subject to the FSO configuration employed.

Operating at lower frequencies offer a higher antenna gain due to the inverse proportionality of the gain of the antenna and the carrier wavelength, as discussed in section 2.3.1. However, higher frequencies can potentially send higher data-rates. By neglecting atmospheric effects (distortion and attenuation), theoretically, data rates are proportional to its carrier frequency. Meaning that

operating at a high frequency provides a better link quality and can potentially send data at a higher rate. Therefore, a rigorous optimization process for the source wavelength of an FSO link is crucial to accomplishing the best execution possible.

The infrared spectrum is classified in different subsections: near IF range 750-1450 nm, which is mostly used for fiber optics due to its low attenuation window. For long-distance links, it is common to use short IR (1400-3000 nm) where the 1530-1560 nm range tends to be used more. For military purposes like guiding missiles, mid-IR wavelengths 3000-800 nm are used, long IR (800 nm - 15 μm) is utilized for thermal imaging and FIR ranges from 15 μm to 1 mm).

The most used bands for wireless communication are radio and microwaves. However, many commercial FSO systems operated near IR and short IR, which have a frequency range on the order of magnitude of 10^{14}Hz. While microwave frequencies are on the order of 10^{9}Hz and 10^{12}Hz, comparing these with IR frequencies, the later can provide a 100-10,000 times higher data rate. IR band also simplify the design process since their components are already available in the market.

Currently, the majority of the optical systems operate in the near-infrared wavelength region (780 nm to 850 nm), mostly due to its cost advantages and availability of effective and reliable semiconductor laser diode sources at that wavelength region. Although cost is undoubtedly a significant factor in the choice of wavelength, one must analyze several additional constraints, like the need to not exceed eye-safe limits on transmitted intensities under conditions of high data-rate transmissions under through heavy atmospheric attenuation (due to fog, rain, storms, etc). Other relevant criteria include overall performance and the potential for system growth and versatility. When all of these factors are considered, it becomes evident that a more exhaustive approach is to operate near 1550 nm, the same wavelength range employed in commercial fiber-optic communications networks.

The range of wavelengths considered for space communication links is 500-2000 nm. A decision is made in the optical design based on the variations of temperature across the Earth's surface and according to the receiver sensitivity and ATP. The following table 4.3 provides an overview of different space communication systems and their wavelengths.

The chosen laser is a 1550 nm coaxial Distributed Feedback (DFB) laser module for digital transmission, CWDM analog communication, and apt for optical networks such as wireless communication links. This cost-effective module has a built-in power monitor photodiode, an optical isolator, and a four pin coaxial pigtailed package with an FC/PC single mode fiber connector.

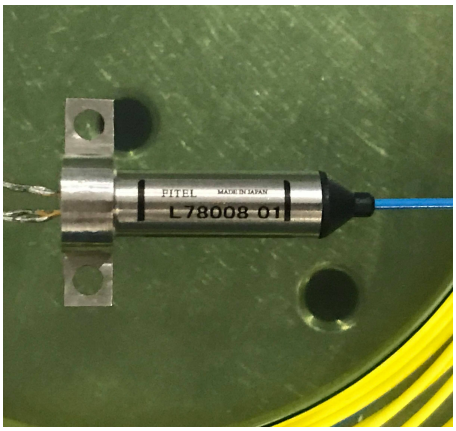

Figure 4.1: Fitel DFB Laser.

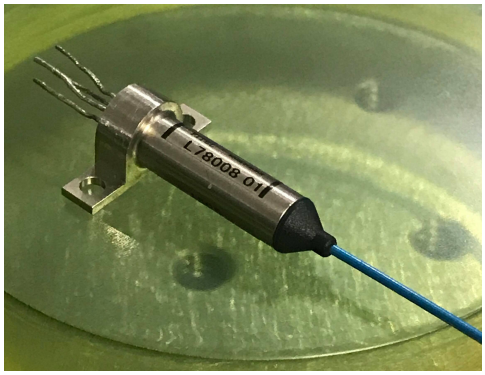

Figure 4.2: Fitel DFB Laser.

Laser Diode Parameter	Min	Typical Value	Max
Threshold Current		8 mA	15 mA
Optical Output Power			2.0 mW
LD Forward Voltage		1.1 V	1.5 V
Peak Wavelength	1530 nm	1550 nm	1570 nm
Spectral Width			1.0 nm
Operational Temperature		25 ° C	

Fiber Type		Single Mode	
Cladding Diameter	122 μm	125 μm	128 μm
Coating Diameter		0.9 mm	
Connector Type		FC/PC	
Dimensions		37x17x8 mm	

Table 4.2: Fitel Coaxial DFB Laser parameter summary

Optical System	Optical Source	Wavelength (nm)	Communication link	Additional parameters
Semiconductor Intersatellite Link Experiment (SILEX) [2]	AlGaAs laser diode	830 nm	Inter-Satellite	60 mW optical power, 25 cm telescope size, 50 Mbps data rate, 6 μrad divergence angle, direct detection
RF Optical System for Aurora (ROSA) [49]	Diode pumped Nd:YVO4 laser	1064 nm	Deep space	6 W optical power, 0.135 m and 10 m transmitter and receiver telescopes size, respectively, 320 kbps data rate
Altair UAV-to-ground Lasercomm Demonstration [50]	Laser diode	1550 nm	UAV-to-ground	200 mW optical power, 10 cm and 1 m uplink and downlink telescopes size, respectively, 2.5 Gbps data rate, 19.5 μrad jitter error
Airborne Laser Optical Link (LOLA) [16]	Lumics fiber laser diode	800 nm	Aircraft and GEO	300 mW optical power, 50 Mbps data rate
Engineering Test Satellite VI (ETS-VI) [7]	Downlink: AlGaAs laser diode Uplink: Argon laser	Uplink: 510-nm Downlink: 830-nm	Bi-directional ground-to-satellite	13.8 mW optical power, 7.5 cm spacecraft telescope size, 1.5m Earth station telescope, 1.024 Mbps bidirectional link data rate, direct detection
Optical Inter-orbit Communications Engineering Test Satellite (OICETS) [5]	Laser Diode	819 nm	Bi-directional Inter-orbit	200 mW optical power, 25 cm telescope size, 2.048 Mbps data rate, direct detection
Mars Laser Communications Demonstration (MLCD) [51]	Fiber laser	1064-nm 1076-nm	Deep space	5W optical power, 30 cm transmitter telescope size and 5m and 1.6 m receiver telescope size, 1-30 Mbps data rate, 64 PPM modulation

Table 4.3: Overview of successful space communication systems

The FSO systems operate in the infrared (IR) range in order to ensure a minimum amount of signal attenuation from scattering and absorption. As mentioned in the previous chapter, FSO

systems operate in the near infrared frequencies from the electromagnetic spectrum (200- 400 10^{12}Hz) mostly around the 850 nm-1550 nm wavelength range [46]. The wavelengths in ranges between 300-500 nm and 800-1400 nm are more susceptible to the atmospheric attenuation than the wavelengths of 850 nm and 1550 nm.

4.1.3 Gaussian beams

This thesis is based on light emitted by a 1550 nm diode laser, operating on the fundamental, TEM_{00} mode (Fig. 4.4). It is, therefore, convenient to begin with a description of ideal Gaussian beams, which is a theoretical description of the lasers' output. Learning about how the laser beam propagates (Fig 4.3) helps to understand the systems' performance.

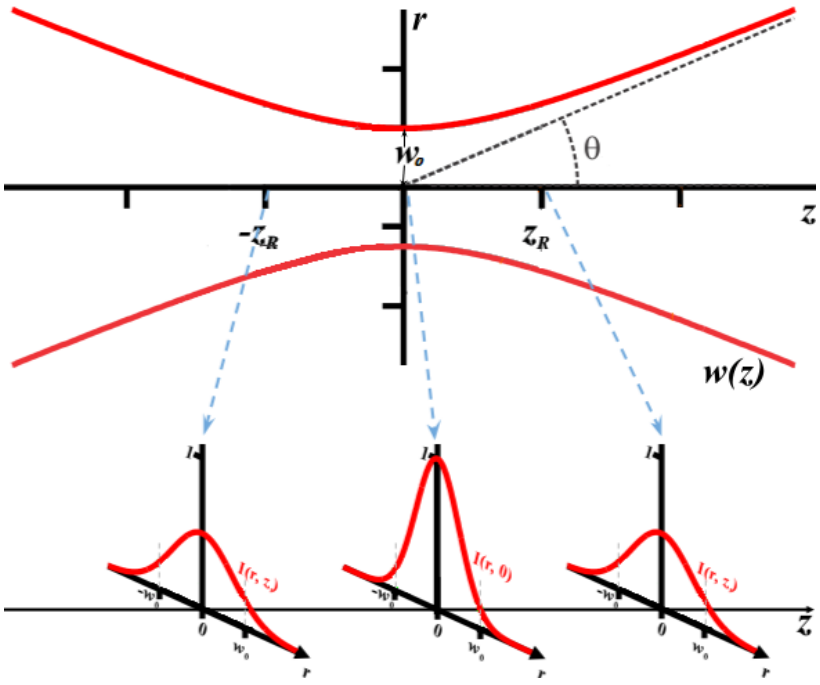

Figure 4.3: Gaussian beam propagation [47].

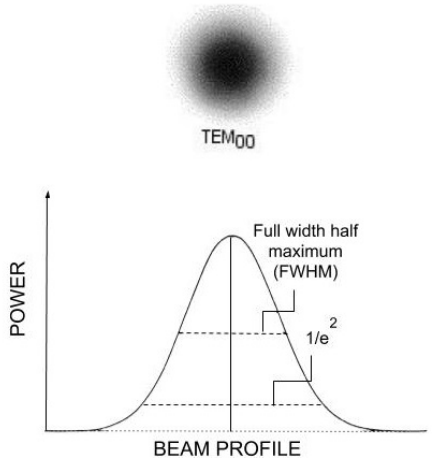

Figure 4.4: TEM_{00} fundamental Gaussian mode [48].

The TEM_{00} mode is the simplest transverse mode of electromagnetic radiation and it propagates with the least beam divergence angle which it is of great desire because it can focus on a narrow spot. Figure 4.4 shows the field pattern of the aforementioned mode. The field pattern is the radiation measured in the plane transverse to the direction of propagation. Mathematically, the Gaussian beam has an amplitude distribution defined by:

$$E(r,z) = E_o \frac{w_0}{w(z)} e^{\frac{r^2}{w(z)^2}} e^{-i\varphi(r,z)} \tag{4.1}$$

where $r = \sqrt{x^2 + y^2}$ is the beam's radial distance and z is the axial distance from the waist beam, E_o= |E(0,0)| is the electric field amplitude at the waist, w(z) is the beam radius (4.3), w_0 = w (0) is the position at which the beam has a minimum size (known as the beam waist) and is generally chosen to be the origin of the coordinate system, last φ(r, z) is the phase. The corresponding optical intensity reads:

$$I(r,z) = |E(r,z)|^2 = I_o(\frac{w_0}{w(z)})^2 e^{-\frac{2r^2}{w^2(z)}} \tag{4.2}$$

with I_o = I (0, 0) being the intensity at the waist.

The beam radius of the light source with a wavelength λ at a distance z is given by,

$$w(z) = w_o \sqrt{1 + \frac{z}{z_R}^2} \tag{4.3}$$

w(z) describes the beam propagating along the transmission path. At this value, the amplitude has dropped to 1/e and the irradiance by $1/e^2$. In addition, the beam radius gives rise to the parameter z_R, called the Rayleigh range. At a distance z from the beam waist, the beam width increases by a factor of $\sqrt{2}$ whereas the intensity on the beam axis decreases to half its peak value.

The Rayleigh range is a distance that describes the behavior of the beam as it propagates. This distance sets a point to where the signal can propagate without diverging significantly. The Rayleigh range its also the value where the beam radius w(z) has increased by $\sqrt{2}$ with respect to the beam waist (w_o). It depends on the beam waist and the carrier wavelength. The Rayleigh range can be expressed as follows:

$$z_R = \frac{\pi w_o^2}{\lambda} \tag{4.4}$$

Similar to w(z) that describes the beam width, there exist other ways to define this parameter, such as referring the spectral width in terms of the Full Width Half Maximum (FWHM), see 4.4 to visualize how the spectral width in terms of FWHM and Gaussian width are related.

Moreover, a narrow spectral width enables more concentrated energy around the carrier frequency. This is one of the main advantages of using lasers. For example, a 1550 nm laser with a 2-nm spectral width has more power concentrated around the carrier frequency than the same signal with 4-nm spectral width. It is useful to understand the beam diameter in terms of the full width at half the maximum (FWHM) values or as the $1/e^2$ intensity criterion (4.4).

4.1.4 Beam Quality

The quality of the beam indicates how divergent is the light emission of a laser diode, this parameter is of greatest interest from an optical design view. The beam quality is dictated by both the laser source (refer to 4.1.3) and collimation optics.

In a perfect world, the transmitted beam of the optical source in a communication system will hit the receiver directly (Figure 4.5). This is just accomplished when the electromagnetic waves from the bearer have a constant phase relationship, implying that the source is fully coherent. Experimentally, the electromagnetic waves of an optical carrier interfere with each other and lead to

the beam to diverge. As outlined in Figure 4.6, when a transmitted signal diverges it forms a cone shape.

Even the best radio and microwave transmitters carry a divergence angle (θ) of a couple of degrees. Contrasted to lasers, where the greater part of them produce light in a very narrow band around a single, central wavelength. Therefore, laser emissions are highly coherent; their beams typically have a divergence of less than a milli-radian (around 0.057 degrees). For instance, an Nd:YAG neodymium laser with a 1064 nm wavelength and a data transfer capacity of 0.00045 microns (0.45 nm), carry a strikingly narrow linewidth of 0.04 percent of the carrier wavelength.

A laser beam with a divergence angle of 0.057 degrees would expand to about one meter in diameter after traveling a kilometer. The areas in which an outsider could distinguish a laser transmission it can be any place inside the volume of the cone depicted before. A highly divergent beam implies that there are more areas in which the transmitted signal could be detected. Additionally, this beam divergence can be substantially reduced by using collimators. Some systems can be designed to have sub-micro radian divergences.

Figure 4.5: Ideal transmission with no beam divergence.

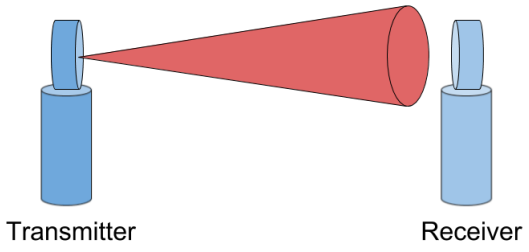

Figure 4.6: Experimental representation of a divergent optical source beam.

4.1.5 Modulation

Modulation is the technique of imposing information on a light source beam and it can be accomplished with a modulator device. This device can be placed externally on the system or directly. There are four main characteristics of the laser beam carrier to send data that can be modulated (i.e. frequency, phase, polarization, amplitude).

Direct modulation imposes a modulation signal in the optical frequency carrier by providing electrical variations proportional to the current or voltage produced, and these signals can be processed by demodulation algorithms. The detection process in an optical communication system consists of converting the variations in the light received by variations in signal voltage, to decode the message.

External modulation modulates the signal after the laser field is generated. This method measures the variations by comparing the modulated signal with a stable phase or frequency from a local coherent reference field. A modulator device like an Electro-Optical-Modulator can be used for external modulation. For the purpose of this thesis, direct modulation is implemented.

4.1.6 Link Establishment

The stability of the beam direction is related to the alignment between the transmitter and received beam in the optical terminal. The alignment cannot be performed during transmission and hence has to be made before the communication starts. The optical devices that are the part of the system have to keep a stable alignment of the optical signal for a given communication period.

4.1.7 Optical Detector

The optical detector is the device that converts the upcoming signal from the transmitter to an electric signal through the photoelectric effect. The electrical signal it is then demodulated to retrieve the transmitted signal.

Although there are many types of detectors (photodiodes, phototransistors, photoresistors, phototubes, photomultipliers, pyroelectric photodetectors, and thermal detectors), in optical communications the most used are the photodiodes. That is because they have the best qualities, like,

small size, high sensitivity, and low cost. The two types of photodiodes employed in practically all optical link systems are the pin photodiode and the APD (Avalanche Photodiode).

Mainly, optical detectors are characterized by two parameters: quantum efficiency and responsivity at a given wavelength. The quantum efficiency is the ability of the device to produce an electron for every incoming photon. Even if the power is constant, not all the percent of photons are converted (Approx. 80 percent is converted) due to the fluctuations in the current by quantum and electric circuit noises. Now, to convert the current to voltage, the trick relies on a transconductance amplifier included in the photodiode.

The quantum efficiency η is given by:

$$\eta = \frac{number\ of\ electrons\ generated}{number\ of\ incoming\ photons} = \frac{I_{PD}/q}{P/h\nu} \tag{4.5}$$

where I_{PD} is the output current from the photodiode, q is the charge of the electron, P is the average optical power received, and hν is the energy for every incident photon.

The second parameter that describes the performance of a photodiode is the responsivity which is the amount of electric current generated by a watt of the incident light power and is given as the ratio of the output current and optical power received by the detector:

$$R(\lambda) = I_{PD}/P = \eta q/h\nu \tag{4.6}$$

The responsivity varies with the material of the photodiode and the wavelength of the input beam. For an FSO system, it is important to choose the detector that has the best responsivity value at the wavelength of the optical source, see section 4. The chosen detector is a junction photodiode, this is a p- and n- device that generates a current flow when the light is absorbed in the InGaAs area of the junction. Based on the upcoming light, it is necessary to be able to determine accurately the expected output current and the responsivity. To attain a better understanding of the main components, characteristics, and operations of a p-n photodiode, figure 4.7 illustrates a junction model.

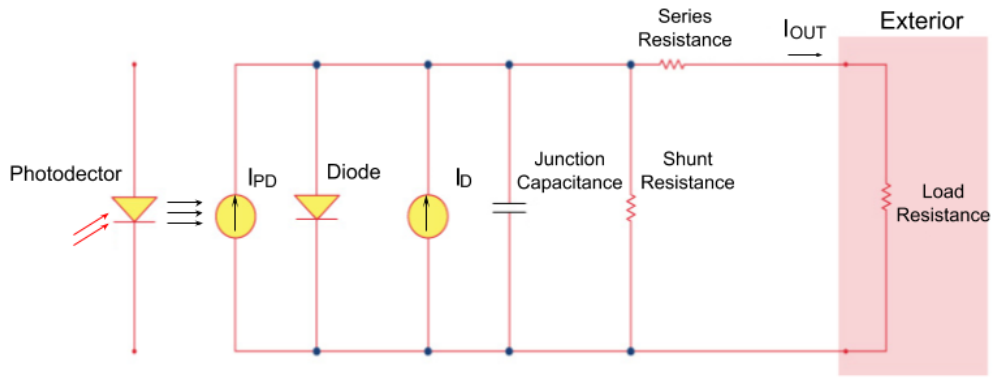

Figure 4.7: Photodiode Model [52]

where the output is terminated by a 50-Ω (R_{LOAD}) resistor and the current is given by the sum of the generated photocurrent and the dark current, $I_{OUT} = I_{PD} + I_D$.

As the photodiode receives the light emission, noises are being generated by diverse factors. One of these constraints is the unwanted current known as the dark current. Dark current is a leak current produced when a bias voltage is applied to the detector. It can raise the temperature of the system and its value depend on the material of the detector and the size of the detection area. The table below enlists the most common types of optical detectors with their corresponding dark currents among other useful parameters.

Material	Spectral Range	Dark Current	Speed	Cost
Silicon (Si)	Visible to NIR	Low	High Speed	Low
Germanium (Ge)	NIR	High	Low Speed	Low
Indium Gallium Arsenide (InGaAs)	NIR	Low	High Speed	Moderate

Table 4.4: Materials of common optical detectors used in FSO systems

Another constraint of photodiodes it is their bandwidth, such parameter depends on various factors. The range of frequencies of a photodiode are in the order of 10^6 to 10^{12} Hertz. As the bandwidth increases, the size of the active area becomes smaller. This is due to the junction capacitance on the detection area, to increase the response speed, the capacitance must be reduced. The junction capacitance (C_J) is an essential property of an optical detector, as it has a significant effect on the data transmission and response.

Type of Detector	Responsivity (A/W)	Operating Voltage (V)	Commonly used for
PIN diode	0.5-0.7	Low	Short link distances
APDs	20-80	Higher	Long link distances

Table 4.5: Common type of optical detectors

The bandwidth constraints the transfer speed of data that can be achievable in a communication link. Hence, it is essential to have a broad knowledge of such characteristic. Two important parameters to measure the bandwidth of a photodiode is the rise and fall time of the detector. The rise and the fall time of a photodiode show that there is a slow drop in the output level after a specific frequency value. The time when the output has dropped to half of its low-frequency value is known as the 3-dB point. At this point, half of the optical power is changed to current contrasted with bring down frequencies. The 3-dB point characterizes the receiver bandwidth. To limit the bandwidth, a load resistor R_L feeds the signal and interacts with the junction capacitance. The bandwidth (f_{BW}) is related to the load resistance (R_{LOAD}) and the junction capacitance (C_J).

$$f_{BW} = \frac{1}{2\pi\, R_{LOAD}\, C_J} \tag{4.7}$$

In the event that the rise and fall times are equal, the 3-dB bandwidth capacity can be evaluated from the rise time t_r by,

$$f_{BW} = \frac{0.35}{t_r} \tag{4.8}$$

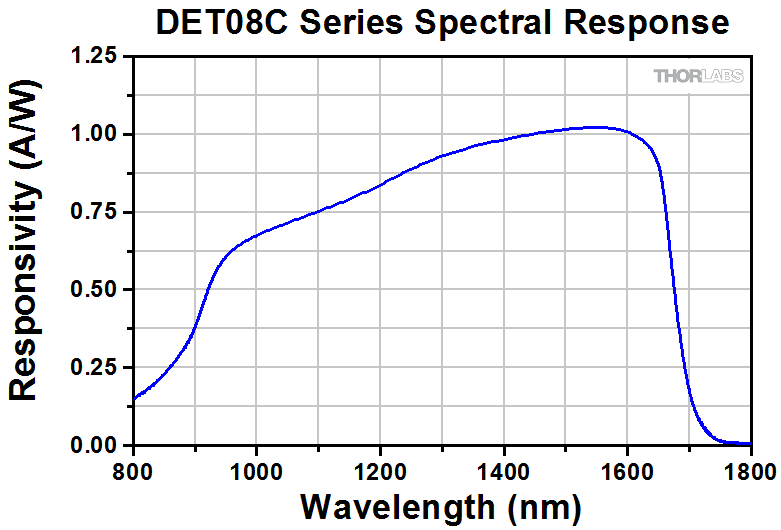

Figure 4.8: Spectral Response of DET08C THORLABAS InGaAs Photodetector [52].

Optical Detector Parameters	THORLABS DET08CFC/M
Wavelength Range	800-1700 nm
Material	InGaAs
Bandwidth	5 GHz
Peak Response	0.90 A/W
Fiber Input Connector	FC/PC
Signal Output Connector	SMA
Min. Load Resistor	50 Ω
Max. Peak Power	100 mW
Max. Output Voltage	2 V
Rise Time t_r	<70 ps at 1538 nm
Fall Time t_f	<70 ps at 1538 nm
Bias Voltage	12 V
Dark Current	1.5 nA
Max. NEP	2x10^{-15} W/$\sqrt{Hz}$ at 1550 nm
Junction Capacitance	0.3 pF
Operating Temperature	0° to 40°C

Table 4.6: THORLABS Fiber-coupled photodiode specs [52]

4.2 Noise

In this section, a discussion of the noises that limit the performance of our signal by the photodiode is given.

4.2.1 Johnson noise

The Johnson or thermal noise results from the thermal variations in conductive devices. It's generated from the fluctuations of electrons in a conductor. The electrons are moving constantly, colliding with each other and with the atoms of the material. Each motion of an electron between collisions creates a voltage difference that will charge the junction capacitor of the photodiode. The thermal noise can be calculated using:

$$I_{JN} = \sqrt{\frac{4k_B T \Delta f}{R_{SH}}} \tag{4.9}$$

where k_B is the Boltzmann constant, T is the temperature in Kelvin, Δf is the noise bandwidth, and R_{SH} is the shunt resistance of the receiver.

To reduce the magnitude of Johnson noise, one may cool the system, specifically the load resistor. Although, reducing the value of the resistor you risk the quality and availability of your signal. The bandwidth should be kept at a small value (e.g. 1-Hz value is regularly applied).

4.2.2 Shot noise

The shot noise arises from the variations in the flow of electrons in a vacuum tube. These fluctuations create noise because of their random arrival of electrons at the anode in the detector. Additionally, unwanted dark current also adds noise to the signal. Thus, we can define the magnitude of the shot noise as:

$$I_{SN} = \sqrt{2q(I_P + I_D)\Delta f} \tag{4.10}$$

q is the electron charge, I_P is the current photo-generated and I_D is the dark current of the photodetector.

4.2.3 Noise Equivalent Power

The noise equivalent power is the amount of power of the incident light hitting the fiber-coupled photodiode. This light generates a photo-current equal to the noise current. NEP is defined as:

$$NEP = \frac{I_{SN}^2}{R} \tag{4.11}$$

To minimize the shot noise one might keep the current value small for any DC component, as well as, the amplification bandwidth low.

Technical noise like Johnson noise and NEP can be suppressed but shot noise is the fundamental limit for detecting signals.

4.3 Optical Design

The purpose of the optical design is to produce a suitable beam divergence matching a desired beam diameter at the receiver. By adding optics to the design, it minimizes the beam divergence along the transmission path. We have used two collimators to ensure a minimum spot size as regards to the transmitter.

It is desired to maintain a Gaussian beam profile along the path of propagation. Doing so provides several advantages (i.e. easier alignment, as the max. power density is in the center of the beam and it is easier to measure the energy at the receivers' aperture).

4.3.1 Fiber Characteristics

In 1970 at Corning Glass in the USA, the scientists Kapron, Keck, and Maurer delivered effectively silica fibers with a 17 dB per kilometer loss, using a 633 nm carrier wavelength. From that point, this innovation has progressed enormously in a short time-frame.

The United States started getting "fibered" in the early eighties. Around that time, communication systems operated commonly at 90 Megabits per second. At this rate, a mode single optical fiber could handle almost 1300 simultaneous voice channels. Today, systems operate at 10 Gb/s and higher. This turns to over 130,000 simultaneous voice channels.

Optical fibers offer a major advantage in the infrastructure of telecommunication links. Fiber optics can facilitate many configuration systems, from short-distance, long-haul links to inter-satellite and ground-to-satellite systems. Fibers possess great qualities such as low attenuation and a high bandwidth capacity. These qualities make fiber optics an ideal candidate to carry high

transmission data (in the order of Gigabits and higher).

A fiber optic cable consists of three sections: the core, cladding, and coating. A typical single mode fiber cable has a 8-μm diameter cylindrical core. The core carries the optical signal and has a high refractive index (n_1). The cladding makes sure that the signal is contained in the core and has a slightly lower index of refraction (n_2), and the coating is composed of a material that protects the glass.

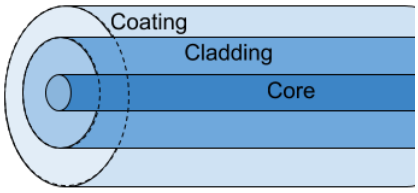

Figure 4.9: Single mode fiber schematic

The guidance of the light beam along the optical fiber is due to the total internal reflection. The total internal reflection is a phenomenon that occurs when an incident beam interferes with two different indexes of refraction (e.g. air and glass). Thus, the light rays traveling in an optical cable are trapped inside the core of the fiber.

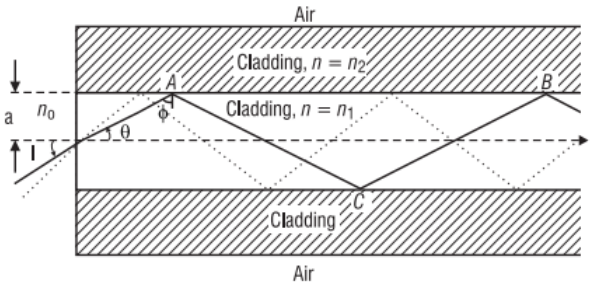

Figure 4.10: A light beam undergoing total internal reflection inside a single mode fiber optic cable [53]

There are three common types of fiber used for optical communication: step-index single mode, multi-mode, and graded-index. The focus of this thesis will be only for single mode fibers. For further understanding, refer to Figure 4.11.

Single-mode step-index fiber, the lowest order mode, allows just a single ray or path for light to travel inside the fiber. For applications where low signal loss and high data rates are required,

single mode fibers are a suitable candidate. This fiber does not experience modal dispersion like the multi-mode type, thus, it can be used for higher bandwidth applications. However, chromatic dispersion limits the performance at higher data rates and long-haul applications when using single-mode fiber. This complication can be overcome by several techniques. One approach is to transmit at a wavelength in which the glass has a moderately constant index of refraction (e.g. 1300 nm), employ an optical source with a very narrow output spectrum, use a low dispersion fiber, or combine all of these methods. In a summary, single-mode fiber is used for high-bandwidth, long-distance applications such as long-distance telephone lines, and high-speed local and wide area network (LAN and WAN) backbones. The major deficiency of single-mode fiber is that it is somewhat complex to work with (e.g. splicing and termination) because of its small core size. To have an idea, the core diameter of an ordinary single-mode fiber is between 5 μm and 10 μm with a 125-μm cladding. Frequently, single-mode fiber is used only with laser sources in view of the high coupling losses related to LEDs. The following table shows the basic parameters of fiber optic cables.

Here the numerical aperture (N.A.) is a measure of how much light can be gathered by an optical device, V is the normalized frequency (or the V-number), which associates the size of the fiber, their refractive index, & the wavelength and Δ is the relative refractive index difference between the core and cladding.

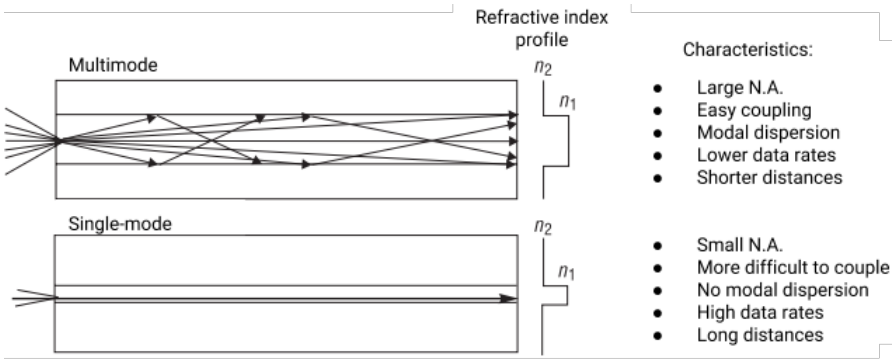

Figure 4.11: Common types of fiber for telecommunications [53]

Optical Fiber Basic Parameters	
Core radius	a
Core index of refraction	n_1
Cladding index of refraction	n_2
Numerical Aperture	$NA = \sqrt{n_1^2 - n_2^2} = n_1\sqrt{2\Delta}$
Normalized index difference	$\Delta = n_2^2 - n_1^2/2n_1^2$
Normalized frequency	$V = \frac{2\pi}{\lambda}\sqrt{n_1^2 - n_2^2} = \frac{2\pi}{\lambda}NA$

Table 4.7: General parameters of fiber optic cables

4.3.2 Collimator specifications

As previously discussed, the field distribution of a single-mode fiber can be approximated by a Gaussian shape. This beam profile creates a wider waist, thus a larger divergence is experienced. To reduce this parameter collimators are added to the system.

A collimator is a device that transforms the diverging light of a radiation emission from a point source to a parallel beam. The narrow beam shape of light enabled by the collimator concentrates the energy of the optical source facilitating efficient communication links. The beam can be used for undercover operations since it is hard to detect it without intercepting it. The disadvantage is that positioning the beam requires a high degree of precision. The optical design involves determining the specifications of the collimator, which involve the focal length, numerical aperture based on the beam diameter and the divergence angle. The choice of collimator takes into account various requirements such as chromatic aberrations, optical field, and wavefront errors, very demanding.

Figure 4.12 shows the collimator assembly of the F220FC-1550 THORLABS, one of the collimators used in our setup. The collimator has a fully AR-coated aspheric lens for a specified wavelength (1550 nm, in this case) and an FC/PC connector at the end. See the table below for detailed information about the optical device.

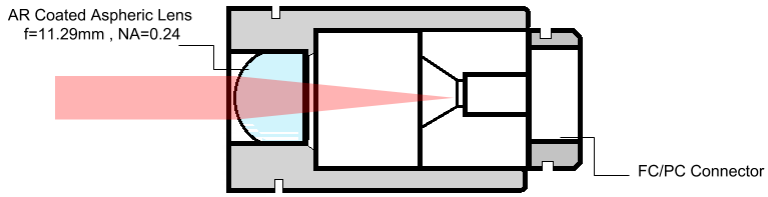

Figure 4.12: Collimator Design.

THORLABS Collimator F220FC-1550	
Alignment Wavelength	1550 nm
Focal Length	11.29 mm
Collimated Beam Diameter - $1/e^2$ output	2.1 mm
Theoretical full-angle beam divergence	0.053°
Fiber Input Connector	FC/PC

Table 4.8: Collimator specifications

The theoretical beam divergence angle when using the fiber collimator at its design wavelength with the fiber Single Mode Fiber (SMF)-28-J9 for 1550 nm. A plot of the theoretical divergence angle over a range of wavelengths is also available in the specifications table below. This divergence angle is easy to approximate theoretically using the formula shown below as long as the light emerging from the fiber has a Gaussian intensity profile. This works well for single mode fibers, when the F220FC-1550 collimator is used to collimate the 1550 nm light emerging from an SMF-28-J9 fiber with a mode field diameter (D) of 3.5 μm and a focal length (f) of approximately 11.29 mm, the divergence angle is approximately given by

$$\theta = (\frac{D}{f})(\frac{180}{\pi}) \tag{4.12}$$

The beam divergence of this collimator was measured for the with a single mode fiber (SMF-28-J9) with a laser operating at 1550 nm. The divergence angle result in 0.0541 degrees. These values are only for an optical system, real measurements are subject to alignment.

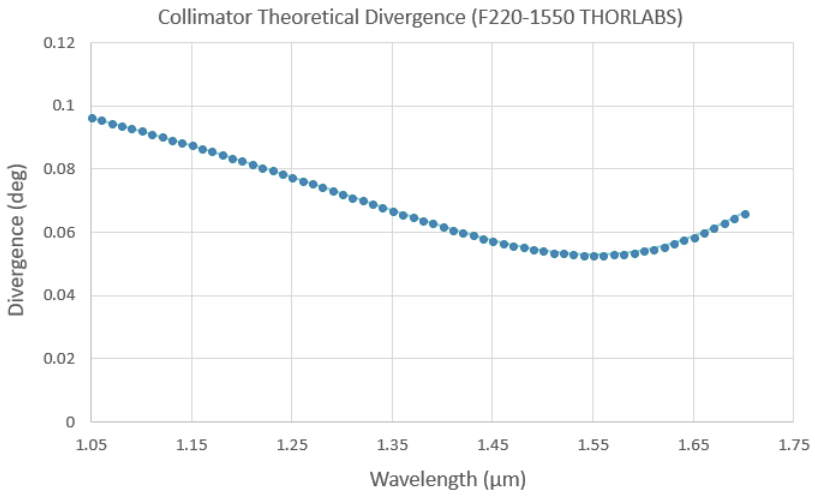

Figure 4.13: Beam divergence as a function of operating wavelength (THORLABS collimator).

The other collimator used has the same properties but a different focal length (4.9-mm). See the table below for detailed information about the optical device.

THORLABS Collimator F220FC-1550	
Alignment Wavelength	1550 nm
Focal Length	4.67 mm
Collimated Beam Diameter - $1/e^2$ output	0.9 mm
Theoretical full-angle beam divergence	0.128°
Fiber Input Connector	FC/PC

Table 4.9: Collimator specifications

4.3.3 Eye Safety

A laser produces an intense highly directional light radiation that can severely damage the human eye if exposed directly or to a reflected beam. The eye is extremely sensitive and will absorb the laser light. This powerful emission will raise the temperature of the cornea (surface of the eye), as well as its interior. Laser exposure will potentially cause an alteration or deformation to the eye. Certain safety measures have to be followed to reduce health risks. The skin can also suffer an injury by a laser beam even with the protection of a layer of cells to overcome some environmental exposures.

Wavelengths between 400 nm to 1500 nm can produce potential eye hazards or damages to the retina, according to the Laser Institute of America (LIA) Laser Safety Information [54]. Therefore, the operating wavelengths for FSO communications have to be safe for the eye and skin. The International Electrotechnical Commission (IEC) classifies lasers into four groups/classes depending on their power and hazards [55]. The vast majority of FSO systems utilize Class 1 and 1M lasers. To have a better understanding, if an FSO system operates at 1500 nm it can transmit more than ten times the optical power of a system operating at shorter wavelengths (e.g. 750 nm). That is due to the way the surface of the eye retains the energy of the light, at 1550-nm the human eye (compared to shorter wavelengths) does not let the retina to focus. An individual can be exposed to a beam with no negative health effects, according to a certain laser power specified by the maximum possible exposure (MPE) [56].

4.4 Modulation Schemes

The data rate that can be transferred in a free space optical system does not depend entirely on the frequency of the signal applied. A lot rests on how information is encoded within the signal, that is, the modulation scheme.

An optical communication system involves the transmission, detection, and demodulation of the optical signal. In FSO communication systems, the intensity of an optical source is modulated to transmit signals over the free space channel. The amplitude, frequency, phase, and/or polarization of the optical signal can be modulated. There are different modulation schemes suitable for FSO systems. The modulation scheme should be chosen based on the power efficiency, bandwidth efficiency, simple design specifications, and low-cost implementations [4]. An FSO modulation scheme depends mainly on two characteristics: optical power and bandwidth efficiency.

4.4.1 AM versus PM

Amplitude Modulation (AM) and Phase Modulation (PM) are two techniques employed to modulate light signals. Both methods can transmit information in the form of electromagnetic waves (analog) or as digital data. AM varies the amplitude of the signal transferred according to the

information being transmitted with a constant phase. This differs from PM in which the information is encoded by varying the phase of the wave with a constant amplitude.

The most common and simple modulation scheme used in free space communication is intensity modulation by direct detection. For example OOK, where the laser is driven with a threshold current then modulated for transmission of data. In the following section, we briefly discuss OOK and another scheme that combines amplitude and phase modulation (i.e. QAM).

4.5 OOK and QAM

The detection process in an optical communication system is required to convert the variations in received light to variations in signal voltage, in order to decode the message. For the most part, FSO systems employ on-off keying (OOK) modulation. In OOK, modulation a binary "1" symbolize that the signal is present while a binary "0" means that the signal is absent. This constrains the rate of information transmission by only sending the signal one bit per period. Another type of modulation is the Quadrature Amplitude Modulation (QAM), which combines amplitude modulation and phase shift keying to attain higher data rates over a single carrier frequency. A QAM receiver requires to be capable of differentiating between signals that have small differences in amplitude and phase. As a result, these signals are more susceptible to noise as a small change in amplitude or phase of the signal may cause the receiver to misinterpret the received data. For this discussion, it is essential to comprehend that QAM can send more information of the carrier signal each period because the varied amplitude and phase of the laser beam enables each signal to represent a progression of binary digits as opposed to only a single bit.

For instance, 4-QAM modulation is where there are four combinations of amplitude and phase of the signal, and along these lines, every symbol represents two binary digits (since 2 bits can represent 4 levels). Accordingly, 4-QAM can theoretically send 2 bits for each symbol it transmits. A 64-QAM, which is a common modulation scheme for microwave frequencies, uses 64 combinations of amplitude and phase, and in this way every symbol in the 64-QAM scheme represents 6 bits. Therefore, 64-QAM can send 6 bits for each symbol it transmits. Microwave spectrum is generally restricted to 64-QAM or (sometimes) 128-QAM. Taking into account that by

increasing the number of levels of QAM makes the signal more susceptible to noise.

Compared to modulation technologies like OOK, QAM-alike schemes use more efficiently the transmission capacity. In this way, the max. data rate that an EMR signal can accomplish does not depend exclusively on the signal's frequency. A laser signal cannot be said to be capable of sending a determined amount of data at a certain time quicker than a microwave transmission only because the frequency of the signal is higher. Due to the way lasers are produced, it is difficult to apply advanced modulation techniques like QAM. If this were accomplished, lasers should be able to attain greater QAM levels than microwaves as a result of their high signal-to-noise ratio. This will be discussed further in the section on bit error rate (BER). There are researchers who say that applying more bandwidth-efficient techniques to lasers is not necessary because of the wide bandwidth available to lasers. Besides, lasers are unlikely to interfere with other laser signals because of their small beam spread. Therefore, research for bandwidth-efficient modulation for lasers is not of high interest.

4.6 Bit Error Rate

BER stands for bit error rate or bit error ratio and it measures the error bits with respect to the total number of bits transmitted, received, or processed (e.g. a BER with a value of 10^6 means that one erroneous bit is received every time a million bits are transmitted). Numerous studies have reported (often by FSO suppliers) that FSO systems typically have lower BER than other radio frequency (RF) communication networks. This information may delude a reader to assume that FSO is a better technology than other RF technologies. In reality, the BER from a system does not rely upon the technology alone. It depends on the quality of the transmitted signal; the distance between transmitter and receiver, the power used by the transmitter, weather conditions, the size and sensitivity of the receiver, the electronics involved, and so forth. For instance, a specific FSO system might indicate to have a much lower BER than an RF system but the FSO system might only operate over 1 km, while the RF system works for over 5 km. In the event that rather, the FSO transmitter and receiver were set 5 km apart, the BER on the FSO system would likely experience a considerable higher BER than that of the RF system. There's also the case where an FSO system

may be specified to have a lower BER than an RF system, and both operate over the same distance. This might be valid on a clear day but not in the event of atmospheric effects (fog, rain, etc). Once again, the FSO system is likely going to encounter a much higher BER than the RF system.

It is essential to indicate that the BER values given for a communications network are specific to that system. A BER may vary depending on many factors such as distance and weather. One must conduct various BER measurements for different data rates under various weather effects. It is not possible to declare whether FSO or RF systems have better BER.

FSO systems do have a quality that enables them to achieve low BER. This is credited to the spectral width of the optical carrier used in FSO links, which in most cases is much smaller than the ones for RF systems. Spectral width is a measure of the range of frequencies that are transmitted.

CHAPTER V

EXPERIMENTAL SETUP

This project comprises several phases. The details of the system' architecture were covered in the previous chapter. We discussed the process and reasons why we chose the components on our system. Now we will present how we set up the experiment. Two systems will be described: a direct detection setup and an optical transmission in free space setup.

5.0.1 Laser Diode Mount

One of our main objects was to keep our system cost-effective. Hence, we deal with off-the-shelf components. A laser diode mount was needed to connect the light source to the current controller source and power the laser. We built our own mount which connects to the current source via a sub-d-9 connector. By studying the pin arrangement of the laser, the laser mount design was created. See figures 5.1-5.2.

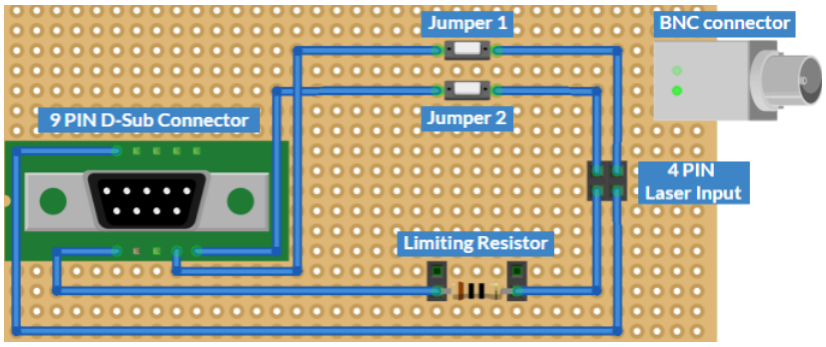

Figure 5.1: Laser Diode Mount Diagram. Breadboard view.

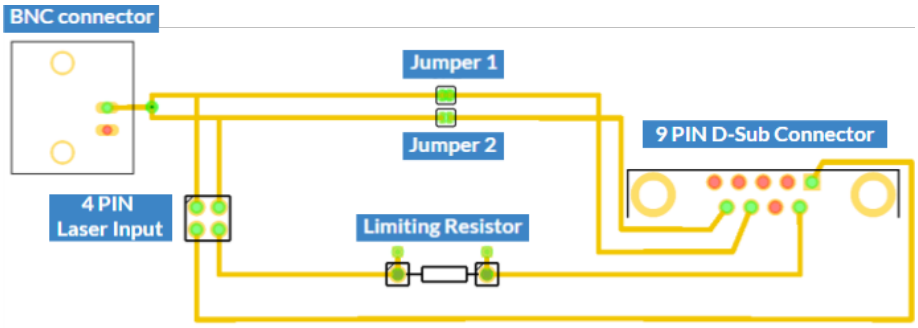

Figure 5.2: Laser Diode Mount Diagram. Circuit view.

The laser mount consisted of a male d-sub-9 pin connector connected to a breadboard where pin 9 & 5 power-up the laser and pin 6 & 7 (See figure 5.6 to see the rear panel arrangement of the laser diode current controller) give access to the built-in laser photodiode. A BNC connector is placed to monitor the photodiode response. In addition, a resistor (limiting resistor) is added to avoid saturating the laser when the current source goes over the lasers' threshold limit.

The final prototype is shown in the picture below 5.3:

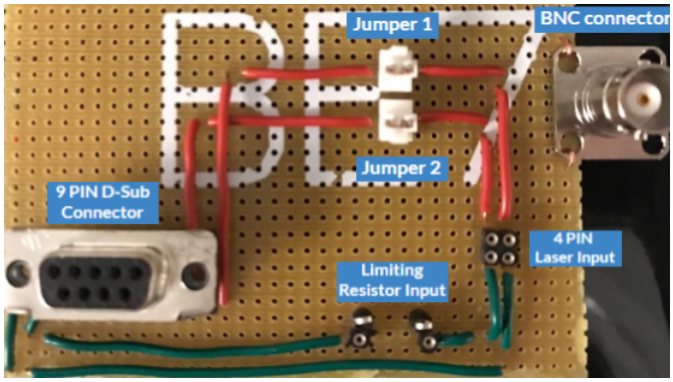

Figure 5.3: Laser diode mount experimental diagram.

5.0.2 Preliminary phase

Our laser arrived without a connector. In order to have an optical source for our communication system, a connect was needed to be spliced to the bare fiber. Basic fiber splicers like the Fujikura FSM-50S Fusion Splicers cost more than 20,000 dollars. After my summer internship at Nokia Bell Labs in 2017, I had the opportunity to network with professors and doctorate students from CREOL, the College of Optics and Photonics at the University of Central Florida. While

attending the Institute of Electrical and Electronics Engineers (IEEE) Photonics Conference in 2017, I was allowed to use the installations at CREOL and fiber splice a connector to the laser. This would not have been possible without the help of Dr. Rodrigo Amezcua and Juan Carlos Alvarado, PhD student.

Fusion splicing is characterized by providing a strong connection with low losses when the fibers are joint. The process consists in stripping the coating of the fibers, cleaving them and clean with alcohol to remove any residues. A dirty bare fiber causes losses in the system and it is difficult for the splicer to align and melt them together. After cleaning, the fiber is aligned within the apparatus and heat is applied via an electric arc. A protective sleeve is added to reinforce the joint.

A fujikura fusion splicer like the one mention above was used to melt together the fiber glass from the DFB laser to a single-mode FC/PC connector. FC/PC is a type of connector that provides a low-loss transmission due to its design (Fig. 5.4). This type of connector allows physical contact between the core of the two fibers connected. Figure 5.5 shows the fusion splicer and the alignment of two fibers before being fused.

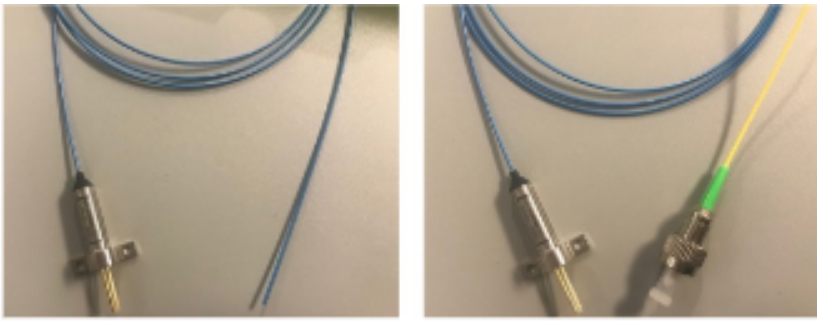

Figure 5.4: Left: DFB Laser without connector. Right: Laser with FC/PC connector.

Figure 5.5: Fujikura Fusion Splicer FSM-50S. Right picture: The ends of the fiber cables are aligned within the splicer before fusion.

Once we had a working laser and laser diode mount, certain measures were taken to handle the light source carefully. We could not afford to lose the only optical source with a connector on it. Hence, we tested a couple of LEDs to make sure that the pin arrangement on the laser mount (5.7) was correctly placed and avoid frying the actual DFB laser. Figure 5.6 illustrates the rear panel output connector of the current controller LDX 3620B and figure 5.7 shows the pin arrangement of the fitel laser.

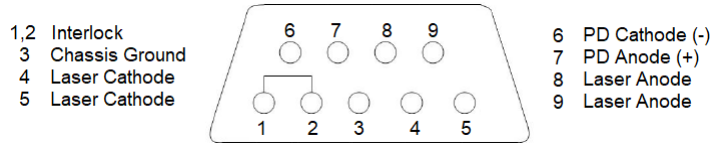

Figure 5.6: LDX 3620B Rear Panel Laser Output Connector.

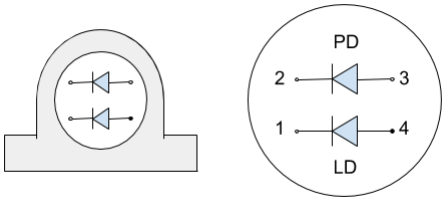

Figure 5.7: Bottom view of laser PIN assignment

5.0.3 Direct Detection Experimental Setup

The setup for a direct detection measurement using direct modulation is presented in the figure below. Detailed information of each component is given in the previous chapter.

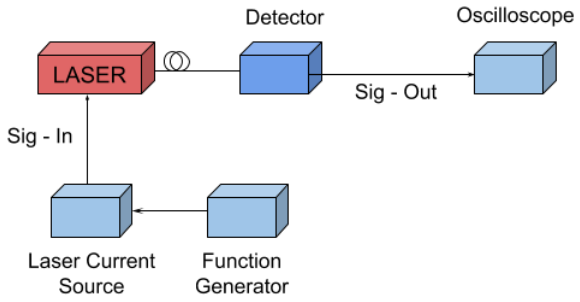

Figure 5.8: Experimental setup for direct detection measurements .

Modulation of the signal was generated using a BK-precision function generator connected to the current source ILX-Lightwave LDX3620B laser diode controller (fig. 5.10). The 1550-nm DFB laser was connected to the LDX3620B via a custom laser mount, refer to Section 5.0.1. The LDX3620B has a transfer function of 2mA/V in the 200 mA range, to avoid saturating the laser, a limiting resistor of 10Ω was hooked to the laser diode mount.

Then the modulated laser output was detected using an InGaAs fiber-coupled photodiode ThorLabs DET08CFC/M and terminated by a 50-Ω load resistor to be observed with a GwInstek GDS-1072A-U oscilloscope. Results are presented in the next chapter.

5.1 Optical Transfer in Free Space Experimental Setup

The second experimental setup has the goal to demonstrate that modulated light can be transmitted and detected along one meter in free space. The experimental setup for such detection is shown fig. 5.9:

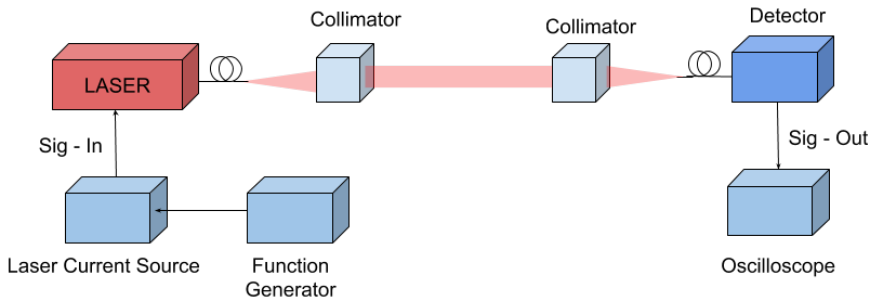

Figure 5.9: Experimental setup for optical transfer measurements.

A standard direct modulation scheme as the one discussed in the previous setup will be used. The function generator imposes a modulation signal to the laser diode via the current source controller. The LDX3620B it is operating again in the 200 mA range. The laser beam output is collimated and the signal is detected by another collimator after one meter of optical transfer in free space. Collimators help to produce a better beam quality. The collimator at the receiver is connected to the fiber-coupled photodiode. The photodiode is terminated by a 50 Ω resistor and measured with an oscilloscope. The specifications for every component are given in Chapter IV.

We set up the components at the Advanced Optics Lab at UTRGV in an optical table bench. Figure 5.11 shows the laser connected to the laser mount to be powered by the laser diode current controller. The laser is then collimated and sent across the optical table. Figure 5.12 shows the other side of the setup where light is gathered by the collimator and coupled into a photodetector to be analyzed by an oscilloscope. Both collimators are set on mirror mounts to facilitate alignment precision.

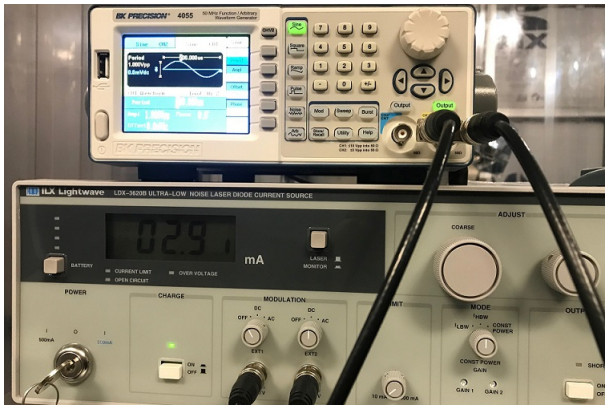

Figure 5.10: Instrumentation part of the experimental setup. Bottom: LDX3620B laser diode current controller. Top: BK precision waveform generator.

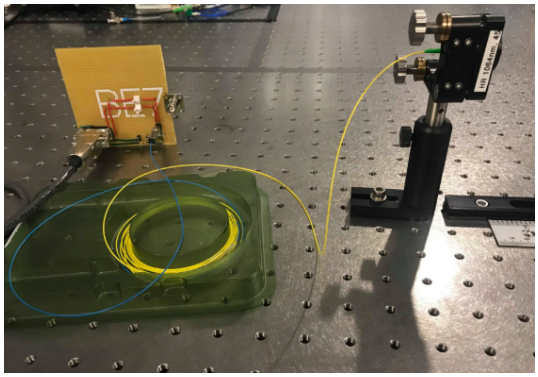

Figure 5.11: Emitter setup.

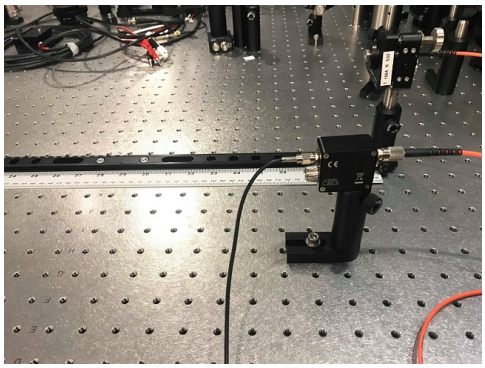

Figure 5.12: Receiver setup.

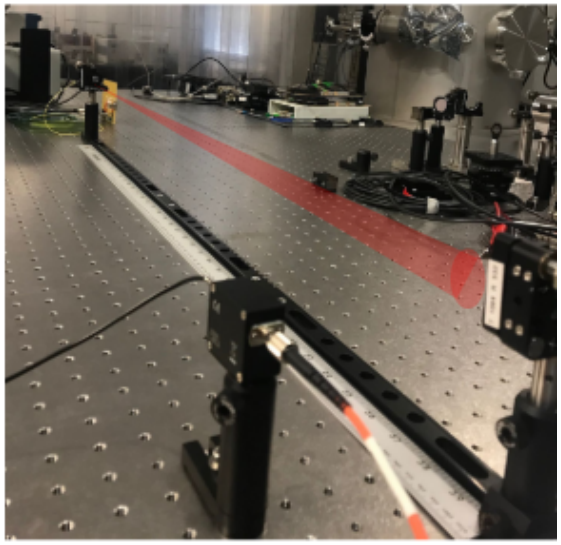

Figure 5.13: Collimated light transmitted in free space over 1 meter and detected with a collimator connected to a fiber-coupled photodetector.

The collimators were mounted on a track to facilitate alignment and variation in propagation distance measurements. The aforementioned, measurements will be performed once we characterize the Gaussian beam propagation of our experimental setup. Results for a direct modulation in one meter of free space for varying modulation frequencies are given in the next chapter.

5.2 Simulation of Design

For a better visualization of the system, a Zemax simulation of the setup design is given. A fiber coupled signal is collimated by a 4.67 mm focal length 1550-nm AR-coated THORLABS collimator, the light is propagated through free space and collimated by an 11.29-mm focal length 1550-nm AR-coated, then detected by the InGaAs fiber-coupled detector. The choice of collimators was based on the availability of the components in the lab when we set the experiment.

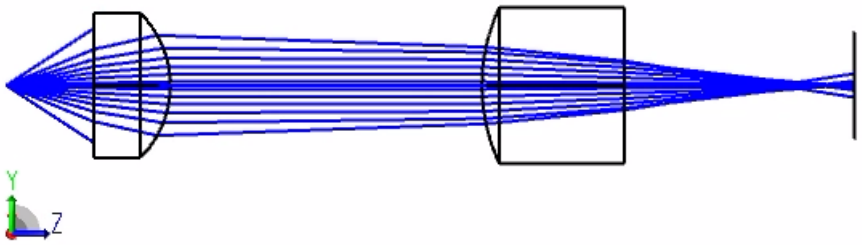

Figure 5.14: Experimental Layout using Zemax.

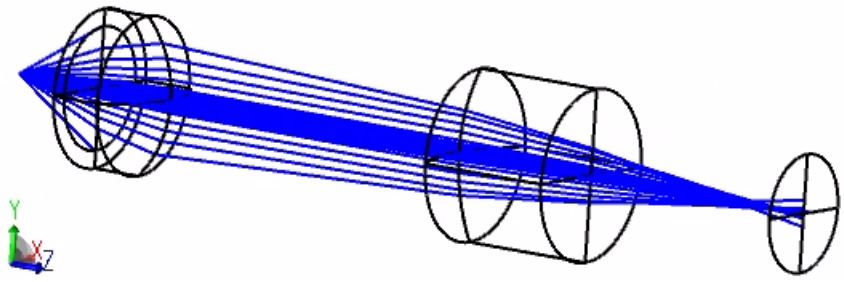

Figure 5.15: 3D Experimental Layout using Zemax.

CHAPTER VI

RESULTS

In this section, we show the results of a direct modulation applied to the carrier laser to transmit information. Two different setups are presented: the laser diode connected to the detector and transmission in free space. A comparison of the signals' performance between the two setups is given.

6.1 Varying the frequency of the modulation wave

We studied the behavior of the modulated output when the frequency of the modulation wave increased from 5-kHz to 400-kHz. The diode current controller was set to the lasers' threshold value of 10-mA with a 100-mVpp amplitude modulating wave. Figure 6.1 shows the experimental setup used for these measurements. The 1550-nm DFB Laser was mounted to the custom laser diode mount (Section 5.0.1) and bias by the LDX3680B. The light source was directly connected to the THORLABS fiber-coupled photodiode with no free space communication. For the photodiode's maximum performance, a 50-Ω coaxial cable and 50-Ω resistor load were connected to the photodetector output [52]. The detected signal was monitored with an oscilloscope. For more details about the experimental setup, refer to the previous chapter.

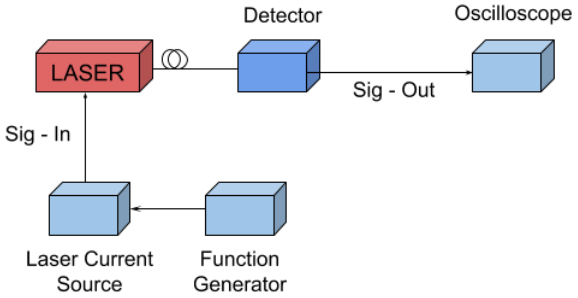

Figure 6.1: Setup for measurements of the light source connected directly to the photodetector .

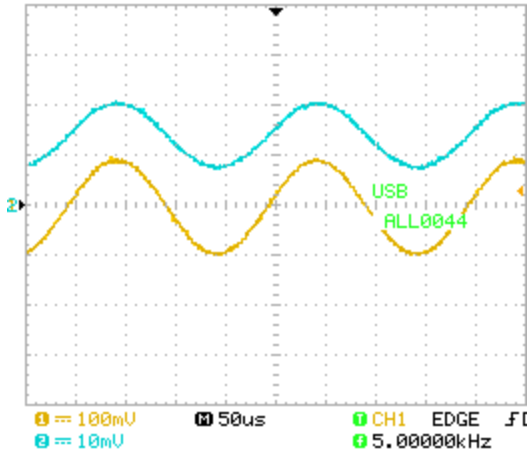

Figure 6.2: Measured voltage response of 1550-nm DFB laser biased at 10-mA with 5-kHz frequency and 100-mVpp amplitude modulation signal.

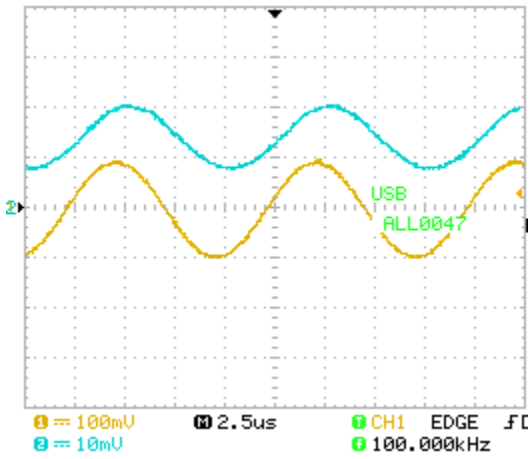

Figure 6.3: Measured voltage response of 1550-nm DFB laser biased at 10-mA with a 100-kHz frequency and 100-mVpp amplitude modulation signal.

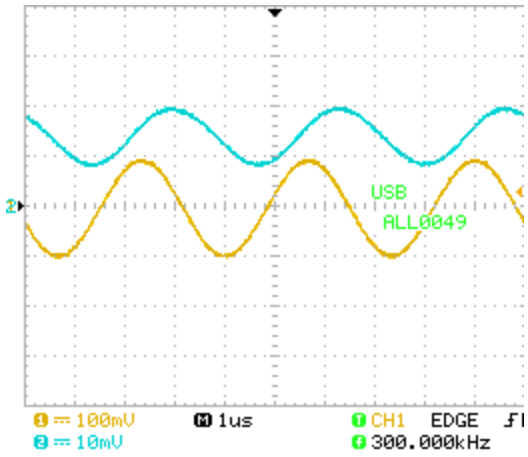

Figure 6.4: Measured voltage response of 1550-nm DFB laser biased at 10-mA with a 300-kHz frequency and 100-mVpp amplitude modulation signal.

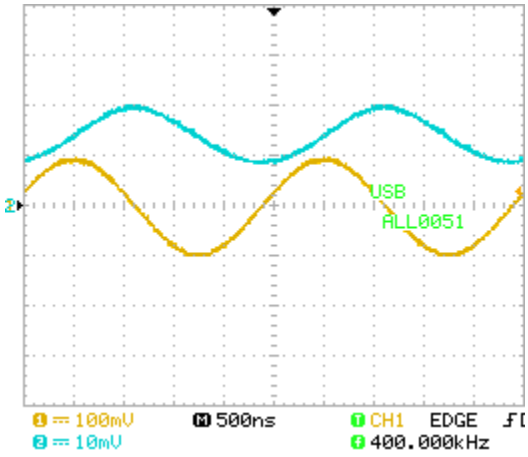

Figure 6.5: Measured voltage response of 1550-nm DFB laser biased at 10-mA with a 400-kHz frequency and 100-mVpp amplitude modulation signal.

Figures 6.2-6.5 show the measured voltage response of a 1550-nm DFB laser operating at 10-mA with a 100-mVpp in amplitude sine modulation signal monitored with an oscilloscope. Channel one is the modulation signal coming from the wave-generator, displayed in yellow, and channel two is the signal modulated and detected by the fiber-coupled photodiode, displayed in blue.

We can also perceive that at 300-kHz the modulated signal has a 45 degrees shift. A low-pass filter with a cut-off frequency of >300-kHz is limiting the modulation bandwidth of our system.

The above measured voltage peak-to-peak for different modulating frequencies are summarized in Table 6.1 and plotted in 6.6 .

Frequency of Modulating Signal	Voltage Peak-to-Peak of Modulated Signal
5-kHz	13.6-mV
100-kHz	12.5-mV
300-kHz	12.0-mV
400-kHz	11.6-mV

Table 6.1: Measured voltage response of 1550-nm DFB laser biased at 10-mA increasing the modulation frequency

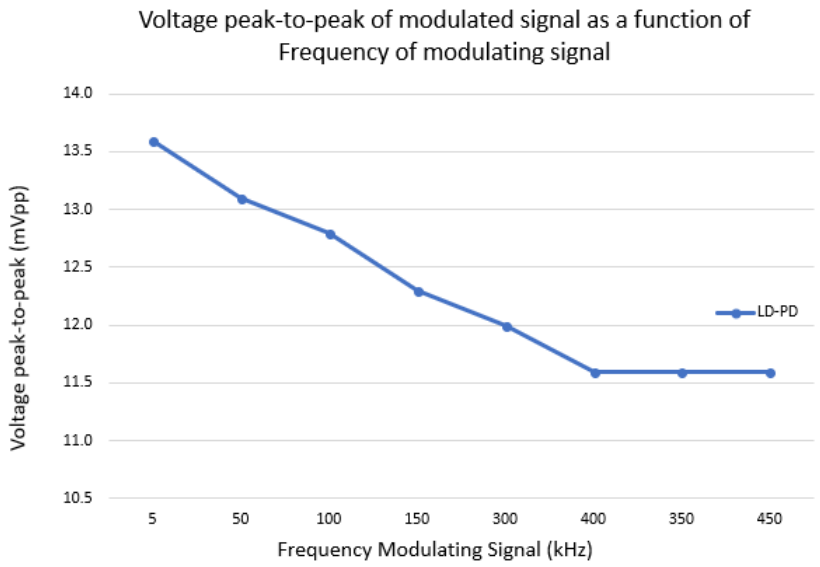

Figure 6.6: Measured voltage response of 1550-nm DFB laser biased at 10-mA increasing the modulation frequency with a constant amplitude modulating signal of 100-mVpp.

The results show that a maximum voltage peak-to-peak of the modulated signal is obtained by setting the laser to 10-mA bias current directly modulated by a sine wave with a 5-kHz frequency and 100-mVpp in amplitude. It is also seen that as the frequency of the modulating signal increases the voltage peak-to-peak decreases. However, from 13.5-mV to 11.6-mV is not a drastic change considering that the modulation frequency was increased from 5-kHz to 400-kHz. Higher frequencies resulted in a saturation of the system.

6.2 Varying the frequency of the modulation wave in Free Space

Once we made sure that measuring a modulated light output was obtained. We proceed to measure the performance of the signal in free space using two collimators on mirror mounts and setting the propagation distance to one meter. The photodiode used was a fiber-coupled InGaAs detector. For more details about the experimental setup, refer to the previous chapter.

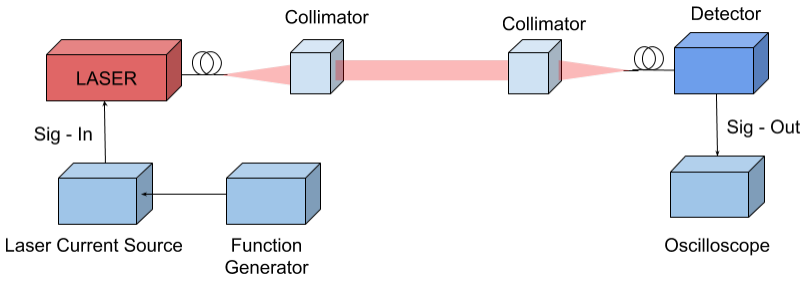

Figure 6.7: Free-Space Communication Measurements Setup.

Figures 6.8-6.11 show the measured voltage response of a 1550-nm DFB laser bias at 10-mA with a 100-mVpp in amplitude sine modulation signal along one meter. The signal was monitored with an oscilloscope.

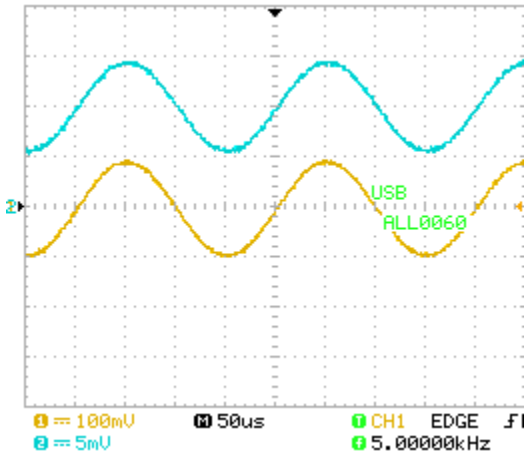

Figure 6.8: Measured voltage response of a 1550-nm DFB laser biased at 10-mA with a 5-kHz modulation signal and measured after one meter of transmission distance in free-space.

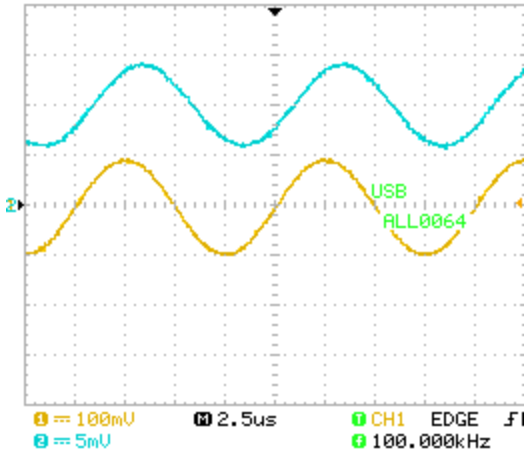

Figure 6.9: Measured voltage response of a 1550-nm DFB laser biased at 10-mA with a 100-kHz modulation signal and measured after one meter of transmission distance in free-space.

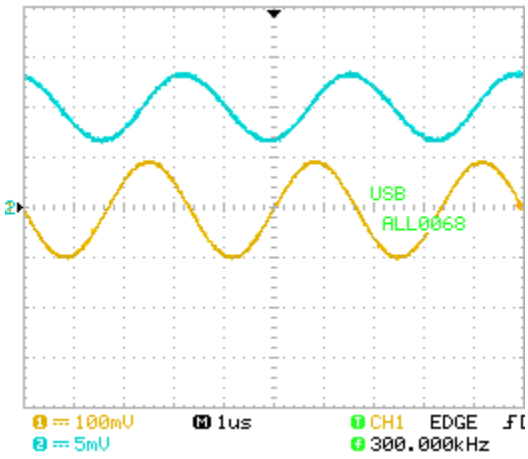

Figure 6.10: Measured voltage response of a 1550-nm DFB laser biased at 10-mA with a 300-kHz modulation signal and measured after one meter of transmission distance in free-space.

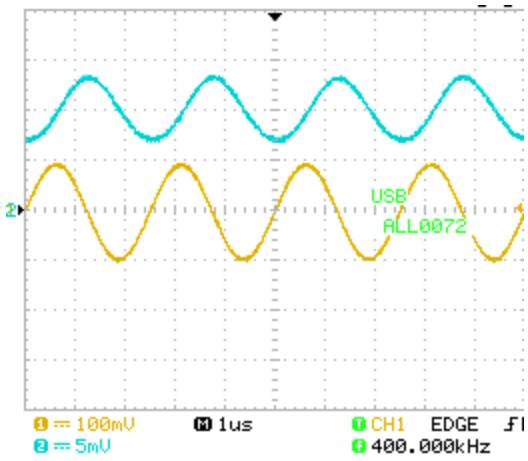

Figure 6.11: Measured voltage response of a 1550-nm DFB laser biased at 10-mA with a 400-kHz modulation signal and measured after one meter of transmission distance in free-space.

The results show that a maximum voltage peak-to-peak of the modulated signal is obtained by setting the laser to 10-mA bias current directly modulated by a sine wave with a 5-kHz frequency and 100-mVpp in amplitude. As we increased the frequency of the modulating signal, the voltage peak-to-peak decreased. A change of 1.8-mVpp between 5-kHz and 400-kHz is observed. The measurements are consistent with the ones from the previous section, we also perceive a 45 degrees shift at 300-kHz in the modulated signal. A low-pass filter with a cut-off frequency of >300-kHz is limiting the performance. Hardware is the source of such limitation.

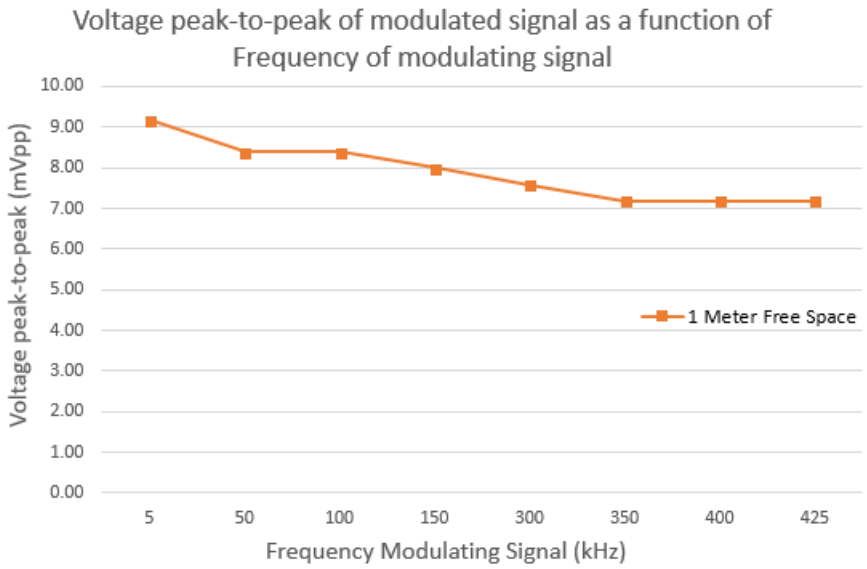

Figure 6.12: Measured voltage response of 1550-nm DFB laser biased at 10-mA increasing the modulation frequency with a constant 100-mVpp amplitude.

Frequency of Modulating Signal	Voltage Peak-to-Peak of Modulated Signal
5-kHz	9.39-mV
100-kHz	8.60-mV
300-kHz	7.19-mV
400-kHz	6.59-mV

Table 6.2: Measured voltage response of 1550-nm DFB laser biased at 10-mA along one meter of free space communication increasing the modulation frequency with a constant amplitude of 100-mVpp.

6.2.1 Comparing the performance of the signal

Figures 6.15 and 6.14 show a comparison of the system's performance when the laser is connected directly to the detector and when there's an optical transfer in free space. For these measurements, the lasers' current was set to 10-mA bias current. The modulation frequency of the sine wave was swept from 5-kHz to 400-kHz with an amplitude of 100-mVpp. For comparison purposes, we are showing the measurements at 300-kHz. The oscilloscope was set to the same parameters to have a better visualization of the comparison.

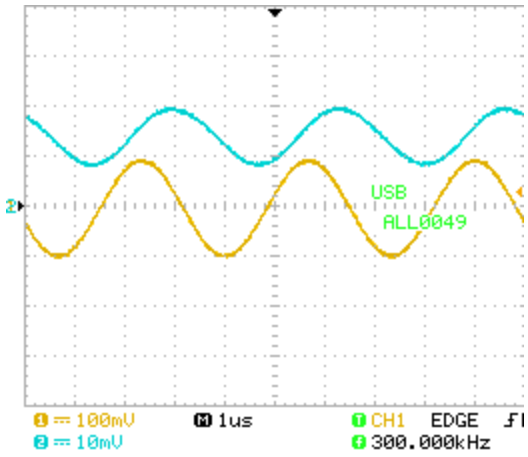

Figure 6.13: Measured voltage response of 1550-nm DFB laser biased at 10-mA with a 300-kHz modulation signal and a 100-mVpp modulating amplitude. The light source is connected directly to the detector.

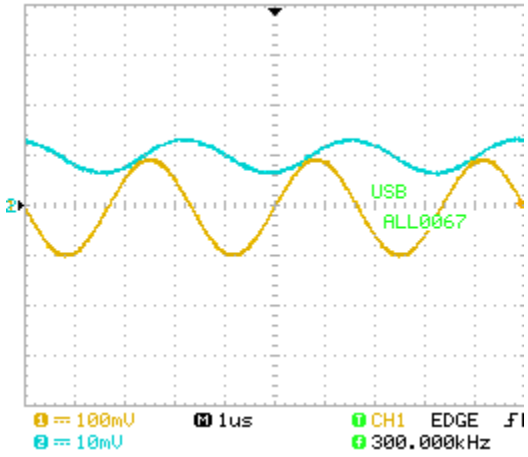

Figure 6.14: Measured voltage response of 1550-nm DFB laser biased at 10-mA with a 300-kHz modulation signal and a 100-mVpp modulating amplitude in free space.

The results of these systems show a significant difference of 4.41-mV voltage peak-to-peak . The losses are expected due to the additional components in the free space communication experimental setup (i.e. the divergence of the light source, atmosphere attenuation, among other losses by the instrumentation).

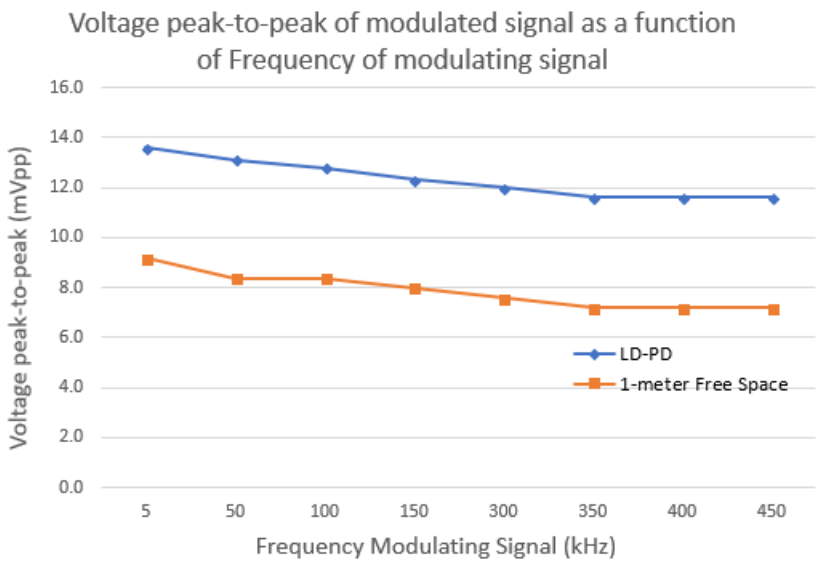

Figure 6.15: Comparison of the measured voltage peak-to-peak of the modulated signal as the modulating signal frequency is increased with a constant modulating amplitude of 100-mVpp.

Frequency of Modulating Signal	Voltage Peak-to-Peak	
	LD-PD	FSO
5-kHz	13.6-mV	9.19-mV
50-kHz	13.1-mV	8.39-mV
100-kHz	12.8-mV	8.39-mV
150-kHz	12.3-mV	8-mV
300-kHz	12-mV	7.59-mV
350-kHz	11.6-mV	7.19-mV
400-kHz	11.6-mV	7.19-mV

Table 6.3: Comparison of the measured voltage peak-to-peak of the modulated signal as the modulating signal frequency is increased with a constant modulating amplitude of 100-mVpp.

In this chapter, the experimental results of a DFB laser modulated with various modulation frequencies measured with two different setups were presented. The results showed that at 5-kHz modulation the system presents it's maximum voltage peak-to-peak and detected power values. In addition, both setups showed a 45-degree shift at 300-kHz indicating that a low-pass-filter must be hidden in the system. Optical transfer in free space using commercially available components is achieved. Although, high modulation frequencies can not be achieved at the moment. An external modulation can be implemented to achieve a high bandwidth communication link.

CHAPTER VII

CONCLUSION AND FUTURE WORK

FSO offers a variety of advantages over the existing radio techniques. The affordable prices and time to set up the system are the main attraction of optical systems. FSO links are suitable for space communication. There are some challenges and limitations, mainly due to the attenuation caused by the propagation medium. However, choosing carefully the parameters and components of the optical communication system can get rid of most of the losses due to the medium.

We set up our FSO system at the Advanced Optics Lab at UTRGV in an optical table to test the systems' performance before installing it at any other location. This has been shown to lead to the improvement of the overall system. A DFB laser diode operating at 1550-nm with an increased of the modulation frequency using two different setups, was studied. The first measurements detected the modulated signal directly from the laser to the detector. In the second setup, the signal was propagated for one meter in free-space. Direct modulation was implemented in both systems. A function generator imposed a modulation signal into the laser through the current source controller and the modulated light output was measured with an oscilloscope.

The experimental results showed that optical transfer in free space for transmission distances up to 1 meter can be achieved using commercially available low-cost components. Moreover, a 45 degrees shift in the signal was observed when the modulating frequency was at set to 300-kHz. Nevertheless, the DFB laser is capable of modulating signals up to 2.5-Gbps and the fiber-coupled photodiode has a 5-GHz bandwidth. Given this information, we concluded that the hardware was limiting the bandwidth of the modulation. Specifically, the current controller source was the source of the limitation in the modulation bandwidth. Both measurements setups were consistent, as they both showed the same response with a 45-degree shift at a 300-kHz modulation frequency.

The work presented in this thesis advances the state-of-the-art by providing the information necessary to continue with the development of a prototype high bandwidth module that can send digital data and receive optical signals to transform them into digital data. As for now, high bandwidth modulation cannot be performed due to the limitations of our laser current diode controller. An external modulator like an electro-optical-modulator can be implemented to achieve a desirable modulation for transmission in space and I will be investigated in the future.

Moreover, the result of this thesis work details the feasibility of and serves as a thorough design handbook for implementing a laser communication system for small satellites with commercially available components. This is a very promising approach for a low-cost setup. It is suitable for space applications and using off-the-shelf components to increase its accessibility.

REFERENCES

[1] G. Oppenhauser, *A world first: Data transmission between European satellites using laser indent light.* ESA News, European Space Agency, 22 November 2001.

[2] *Artemis and SPOT 4 communicating via the SILEX system - Artist's impression.* Released 08/02/2002 4:14 pm. Copyright ESA-J. Huart.

[3] A. Katsuyoshi. *Overview of the optical inter-orbit communications engineering test satellite (OICETS) project.* J. Nat. Inst. of Info. and Comm. Tech., vol. 59, pp. 5-12, 2012.

[4] T. T. Nielsen and G. Oppenhauser. *In-orbit test result of an operational optical intersatellite link between ARTEMIS and SPOT4, SILEX.* Proc. SPIE, Free Space Laser Comm. Tech. XIV, vol. 4635, 2002.

[5] Y. Fujiwara, et al. *Optical inter-orbit communications engineering test satellite (OICETS),* Acta Astronautica, Elsevier, vol. 61, no. 1-6, pp. 163-175, 2007.

[6] M. Toyoda, et al. *Ground to ETS-VI narrow laser beam transmission.* Proc. SPIE, vol. 2699, pp. 71-80, 1996.

[7] K. Nakamaru, et al. *An overview of Japan's Engineering Test Satellite VI (ETS-VI) project,* in Proc. IEEE, Communications, Int. Conf. on World Prosperity Through Comm., vol. 3, (Boston, MA), pp. 1582-1586, 1989.

[8] F. Bellinne and D. E. Tonini. *Flight testing and evaluation of airborne multisensor display systems.* J. Aircraft, vol. 7, no. 1, pp. 27-31, 1970.

[9] R. Miglani. *Free Space Optical Communication: The Last Mile Solution to High Speed Communication Networks.* J Laser Opt Photonics. 2017.

[10] PureLiFi, purelifi.com/technology/

[11] V. G. Sidorovich. *Solar background effects in wireless optical communications.* Proc. SPIE , Opt. Wireless Comm. V, vol. 4873, 2002.

[12] A. Biswas, F. Khatri, and D. Boroson, *Near-Sun free-space optical communications from space.* in Proc. IEEE Aerospace Conf., (Big Sky, MT), 2006.

[13] G. P. Anderson et al. *MODTRAN4: Radiative transfer modeling for remote sensing* Proc. SPIE, vol. 3866, pp. 2-10, 1999.

[14] R. W. Fox, C. W. Oates, and L. W. Hollberg, *Stabilizing diode lasers to high finesse cavities in Cavity Enhanced Spectroscopies* R. D. van Zee and J. P. Looney, eds, vol. 40 of Experimental Methods in the Physical Sciences, pp. 1, 46, Academic Press, 2003.

[15] G. P. Anderson et al. *AFGL atmospheric constituent profiles (0-120 km).* Tech Report, Air Force Geophysics Laboratory Environmental Research Papers, 1986.

[16] V. Cazaubiel, et al. *LOLA: A 40,000 km optical link between an aircraft and a geostationary satellite,* in Proc. 6th International Conf. Space Optics, (Netherlands), Jun. 2006

[17] H. Weichel, *Laser Beam Propagation in the Atmosphere.* SPIE, Bellingham, WA, 1990.

[18] R. K. Long, *Atmospheric attenuation of ruby lasers,* Proc. of the IEEE, vol.51, no.5, pp. 859-860, May 1963.

[19] R. M. Langer, *Effects of atmospheric water vapour on near infrared transmission at sea level,* in Report on Signals Corps Contract DA-36-039-SC-723351, J.R.M. Bege Co., Arlington, Mass, May 1957.

[20] Humboldt Data Hub. *Atmospheric Absorption and Transmission.* http://gsp.humboldt.edu.

[21] F. G. Smith, J. S. Accetta, and D. L. Shumaker, *The infrared and electro-optical systems handbook: Atmospheric propagation of radiation,* SPIE press, vol. 2, 1993.

[22] F. X. Kneizys, *Atmospheric Transmittance/Radiance [Microform]: Computer Code LOWTRAN 6.* Bedford (USA), 1983.

[23] H. Willebrand and B. S. Ghuman, *Free Space Optics: Enabling Optical Connectivity in Today's Networks.* Sams Publishing, 2002.

[24] R. N. Mahalati and J. M. Kahn, *Effect of fog on free-space optical links employing imaging receivers,* Opt. Exp., vol. 20, no. 2, pp. 1649-661, 2012.

[25] J. M. Wallace and P. V. Hobbs, *Atmospheric Science: An Introductory Survey*. Academic Press, 1977.

[26] A. Harris, J. J. Sluss, H. H. Refai, and P. G. LoPresti, *Analysis of beam steering tolerances and divergence for various long range FSO communication links,* Proc. SPIE, Digital Wireless Comm. VII and Space Comm. Tech., vol. 5819, no. 455, 2005.

[27] J. Katz, *Planets as background noise sources in free space optical communiction*. TDA Progress Report: 42-85, Advanced Electronic Material and Devices Section, 1986.

[28] Y. Dong, H. Liu, Z. Luo, Y. Li, and G. Jin, *Principle demonstration of fine pointing control system for inter-satellite laser communication,* Science China Technological Sciences, vol. 58, no. 3, pp. 449-453, 2015.

[29] H. Guo, B. Luo, Y. Ren, S. Zhao, and A. Dang, "Influence of beam wander on uplink of ground-to-satellite laser communication and optimization for transmitter beam radius.," Opt. Lett., vol. 35, no. 12, pp. 1977-1979, 2010.

[30] G. A. Tyler, *Bandwidth considerations for tracking through turbulence,* J. Opt. Soc. Am., vol. 11, no. 1, pp. 358-367, 1994.

[31] H. Hemmati, *Interplanetary laser communications,* in Optics and Photonics News (OSA), 2007.

[32] H. J. Kramer, Observation of the Earth and Its Environment: Survey of Missions and Sensors. Springer, 2002.

[33] M.Heurs. *Gravitational waves in a new light-Novel stabilization schemes for solid-state lasers*.

[34] M. Swartwout, *The first one hundred cubesats: A statistical look.* Journal of Small Satellites, Vol. 2, No.2, pp. 213-233, 2013.

[35] D. Misra, D. Misra and S. P. Tripathi, *Satellite Communication Advancement, Issues, Challenges and Aplications.* International Journal of Advanced Research in Computer and Communication Engineering, vol. 2, no. 4, pp. 1681-1686, 2013.

[36] J. Foust, *How big is the market for small launch vehicles?* SpaceNews Magazine. Spacenews-mag.com

[37] CalPoly San Luis Obispo. *Cubesat design specification*. Technical report, CalPoly San Luis Obispo, Feb 2014

[38] A. Majumdar and J. Ricklin, *Free-Space Laser Communication*. Springer Science and Business Media LLC, 2008.

[39] D. Aviv, *Laser Space Communications*. Artech House, Inc., 2006.

[40] R. W. P. Drever and J. L. Hall. *Laser phase and frequency stabilization using an optical resonator*. Applied Physics B., 31:97, 1983.

[41] R. V. Pound. *Frequency Stabilization of Microwave Oscillators*. Proceeding of the I.R.E, pages 1405-1415, 1947. Applied Physics B., 31:97, 1983.

[42] H. Muller et al. *Tests of relativity by complementary rotating michelson morley experiments.* Physical Review Letters, vol. 99, no. 050401, 2007.

[43] A. Bartels et al., *Femtosecond-laser-based synthesis of ultrastable microwave signals from optical frequency references.* Optics Letters. vol. 30, issue 6, pp.667-669, 2005.

[44] N. R. Newburry, et al. *Coherent transfer of an optical carrier over 251 km.* Optics Letters. vol. 32, issue 21, pp. 3056-3058, 2007.

[45] A. Abramovici, et al. *LIGO: The Laser Interferometer Gravitational-Wave Observatory.* Science. 17 Apr 1992. Vol. 256, Issue 5055, pp. 325-333.

[46] B. Ghuman and H.Willebrand, *Making Free-Space Optics Work,* Sams Publishing, 29 March 2002.

[47] OpenSPIM, *SPIM Optics 101/Theoretical basics.* January 11, 2014.

[48] Schwartz, Dru. *Head and optics innovations key to laser cutting growth*. thefabricator.com. April 4, 2016.

[49] T. Dreischer, et al. *Integrated RF-optical TT and C for a deep space mission,* Acta Astronautica, vol. 65, no. 11, pp. 1772-1782.,2009.

[50] G. G. Ortiz, et al. *Design and development of a robust ATP subsystem for the altair UAV-to-ground lasercomm 2.5-Gbps demonstration,* Proc. SPIE, Free Space Laser Comm. Tech. XV, vol. 4975, 2003.

[51] D. M. Boroson, A. Biswas, and B. L. Edward, *MLCD: Overview of NASA's Mars laser communications demonstration system,* Proc. SPIE, Free Space Laser Comm. Tech. XVI, vol. 5338, 2004

[52] *DET08CFC - InGaAs Photodiode,* Thorlabs, Inc.

[53] Massa, N. *Fiber Optic Telecommunication*. Fundamental of photonics.

[54] O. Bader and C. Lui, *Laser safety and the eye: Hidden hazards and practical pearls.* Tech. Report: American Academy of Dermatology, Lion Laser Skin Center, Vancouver and University of British Columbia, Vancouver, B.C., 1996.

[55] *Safety and laser products- Part 1: Equipment classification and requirements,*International Electrotechnical Commission, (IEC-60825-1), Ed. 3, 2007.

[56] M. Toyoshima, et al. *Assessment of eye hazard associated with an optical downlink in freespace laser communications,* Proc. SPIE, Free Space Laser Comm. Tech. XIII, vol. 4272, 2001.

[57] C.R. Nave , *HyperPhysics,* Department of Physics and Astronomy, Georgia State University, 2003.

BIOGRAPHICAL SKETCH

Andrea Tellez Silva was born in Mexico City, Mexico on April 5, 1994. In 2012, after completing her schoolwork with a perfect GPA at a high school (Preparatoria Ricardo Flores Magon) across the border in Matamoros, Tamaulipas, Mexico she was accepted with a full-ride research-based scholarship at The University of Texas at Brownsville. During her first summer as a college student, she interned at the Laser Interferometer for Gravitational-waves Observatory known for the recent discovery of Gravitational Waves, proving Einstein's Theory of Relativity. In March 2016, she was named the Outstanding International Female Student at her university. She received a Bachelor of Science in Physics with a concentration in Pure and Applied Physics from The University of Texas Rio Grande Valley in May 2016. Then interned at the National Radio Astronomy Observatory in the Charlottesville, Va facilities for ten weeks working with the Photonics Group for the Atacama Large Millimeter Array. In August 2016, she entered the Physics graduate program at The University of Texas at Rio Grande Valley while working as a Physics Laboratory Instructor at her institution. During the summer of 2017, she landed an internship with a well known company founded by Alexander Graham Bell, Nokia Bell Labs in Homdel, New Jersey. Her interests are in photonics, optics, optical networks systems and devices. She received a Master of Science in Physics Degree from The University of Texas Rio Grande Valley in 2018. For further information, contact her at andrea.tellez120@gmail.com